Technical Report Documentation Page

1. Report No.	2. Government Accession No.	3. Recipient's Catalog No.
FHWA/TX-92+1239-2		

4. Title and Subtitle	5. Report Date
AN ULTIMATE LOAD TEST TO STUDY BRACING EFFECTS OF BRIDGE DECKS	May 1992
	6. Performing Organization Code
7. Author(s)	8. Performing Organization Report No.
Swarnalatha Vegesna and J. A. Yura	Research Report 1239-2
9. Performing Organization Name and Address	10. Work Unit No. (TRAIS)
Center for Transportation Research The University of Texas at Austin Austin, Texas 78712-1075	11. Contract or Grant No. Research Study 3-5-90/1-1239
	13. Type of Report and Period Covered
12. Sponsoring Agency Name and Address	Interim
Texas Department of Transportation (formerly State Department of Highways and Public Transportation) P. O. Box 5051 Austin, Texas 78763-5051	14. Sponsoring Agency Code

15. Supplementary Notes

Study conducted in cooperation with the U. S. Department of Transportation, Federal Highway Administration

Research Study Title: "Bracing Effects of Bridge Decks"

16. Abstract

The objective of this research project was to study the possible bracing effect of a bridge deck on the lateral instability of the stringers. The capacity of bridges is frequently underrated due to conservative assumptions regarding unknown conditions. Traditionally, the stringers have been taken to be laterally unsupported along the span, thus leading to conservative estimates of the bridge capacity. A full-size laboratory test was conducted on a 24-foot-span multi-girder bridge comprising five steel stringers supporting a wood deck, to demonstrate the bracing effect of the deck. It was seen that the bridge failed by lateral buckling of the bridge beams. The test bridge capacity was twice the unbraced capacity (assuming no bracing from the deck).

17. Key Words	18. Distribution Statement
bracing effect, bridge deck, lateral instability, stringers, capacity, unsupported, span, conservative, multi-girder, steel	No restrictions. This document is available to the public through the National Technical Information Service, Springfield, Virginia 22161.

19. Security Classif. (of this report)	20. Security Classif. (of this page)	21. No. of Pages	22. Price
Unclassified	Unclassified	70	

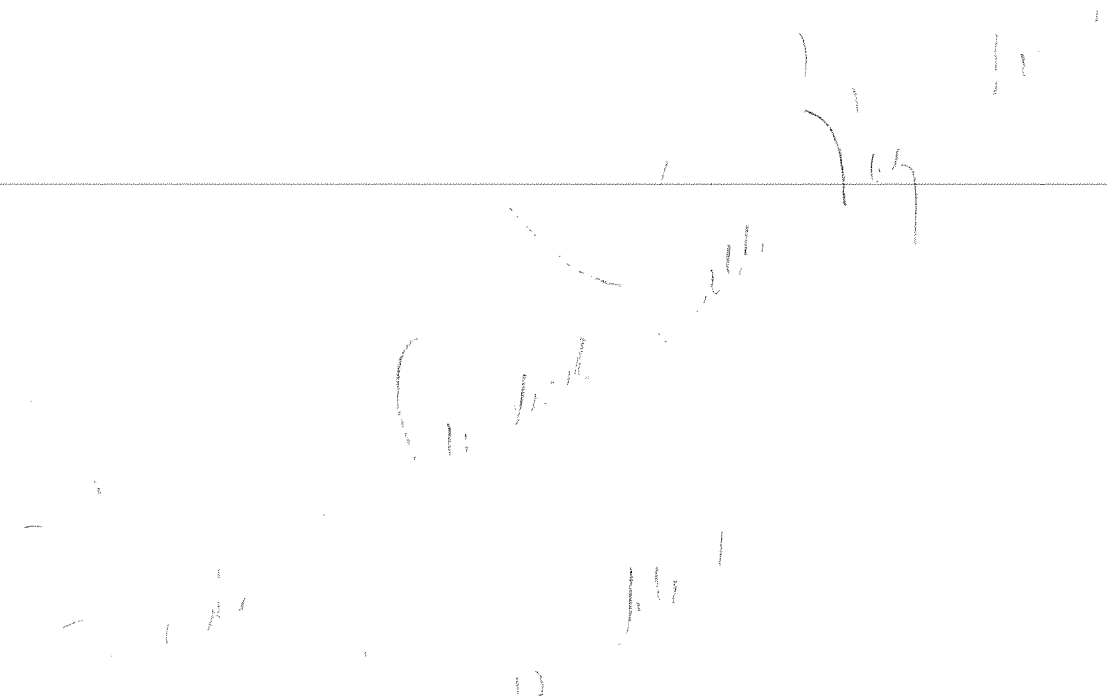

AN ULTIMATE LOAD TEST TO STUDY BRACING EFFECTS OF BRIDGE DECKS

by

Swarnalatha Vegesna and J.A. Yura

Research Report No. 1239-2

Research Project 3-5-90-1239
"Bracing Effects of Bridge Decks"

Conducted for

Texas
State Department of Highways and Public Transportation

In Cooperation with the
U.S. Department of Transportation
Federal Highway Administration

by

CENTER FOR TRANSPORTATION RESEARCH
BUREAU OF ENGINEERING RESEARCH
THE UNIVERSITY OF TEXAS AT AUSTIN

May 1992

NOT INTENDED FOR CONSTRUCTION,
PERMIT, OR BIDDING PURPOSES

Joseph A. Yura, P.E.
(Texas No. 29859)

Research Supervisor

The contents of this report reflect the views of the authors who are responsible for the facts and accuracy of the data presented herein. The contents do not necessarily reflect the official views or policies of the Federal Highway Administration. This report does not constitute a standard, specification, or regulation.

PREFACE

This report documents the results of an ultimate strength test on a full-size single-span steel stringer bridge with a wooden deck. The purpose of the test was to evaluate the bracing effect of the wood deck and the truck on the lateral instability of the stringers. The wood deck was not attached to the steel stringers. Specifically, the question "Is a wheel load location a brace point?" is addressed.

The work reported herein is one phase of Research Project 3-5-90-1239, "Bracing Effects of Bridge Decks." The studies described were conducted at the Phil M. Ferguson Structural Engineering Laboratory as part of the overall research program of the Center for Transportation Research of The University of Texas at Austin. The work was sponsored jointly by the Texas Department of Transportation and the Federal Highway Administration under an agreement with The University of Texas at Austin and the Texas Department of Highways and Public Transportation. Technical contact and support by the Bridge Division was provided by Mark Bloschock.

Page iv

is blank

SUMMARY

A full-scale laboratory test was conducted on a 24-ft span multi-girder bridge comprised of five steel stringers supporting a timber plank deck. The bridge was loaded until failure with a moving load system composed of a standard truck axle and a cart loaded with concrete blocks. Preliminary tests were conducted on individual beams to study single beam behavior. The computer program BASP and design equations were used to arrive at theoretical values. The live load capacity of this bridge, assuming the beams are unbraced, would be zero based on the 1986 AASHTO Bridge Specification.

The bridge failed due to lateral buckling of the five stringers when the 16-kip axle load reached midspan. The five stringers and the deck itself (along with the truck) moved laterally at midspan. The test showed that a wheel load, per se, cannot be considered a brace point. However, the deck provided enough bracing to double the buckling capacity compared to the unbraced case. This bracing effect enabled the stringers to almost reach their yield capacity before buckling. The test bridge was designed to have minimal stiffness.

Page ii

is blank

IMPLEMENTATION

The Bridge Rating Manual needs to be updated immediately to use the new AASHTO 1990 lateral buckling formula. The new formulation gives more realistic capacities compared to older versions of the AASHTO Specification.

The bridge deck tested had minimal stiffness which was not sufficient to fully brace the beams at the load point, but enough to significantly increase the bridge capacity. In other phases of this research project, lateral buckling formulas are developed which consider the effect of any bracing and some typical bridge decks are evaluated.

Page viii

is blank

TABLE OF CONTENTS

LIST OF FIGURES

LIST OF TABLES

Joe —

Three pages from 1239-2 (first report) — these should work with no problem —

Chapter 1
INTRODUCTION

1.1 Background

The capacities of bridges, constructed with steel stringers supporting a timber plank deck or concrete deck which is not positively attached to all stringers, may be underrated by current AASHTO standards. The lateral buckling formula used in the Texas Bridge Rating Manual, which is the same as that in the AASHTO Bridge Specifications prior to 1990, gives very conservative estimates of strength. When there is no positive connection between the stringers and the deck, the beams may be considered laterally unsupported along the span. This yields a load carrying capacity which is much lower than the loads these bridges are known to support. Figure 1.1 is the photograph of a typical bridge; Figure 1.2 shows the deck-beam connection detail.

Figure 1.1 Photograph of a typical bridge

The discrepancy between predicted and actual strength is due in large part to conservative modeling assumptions made by bridge engineers concerning unknown conditions. The apparent observed strength has led to the contention that the deck provides bracing to the steel stringers at the location of the truck wheel.

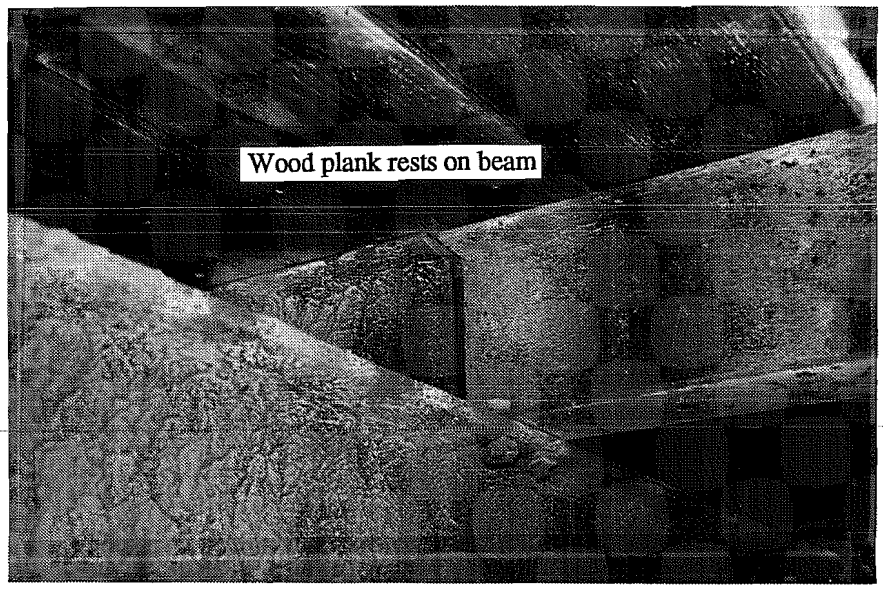

Figure 1.2 Photo of Deck-beam connection

The objective of the research project, sponsored by the Texas State Department of Highways and Public Transportation, was to determine the bracing requirements to increase the lateral buckling strength of beams and to demonstrate the ability of deck material to provide this bracing. Theoretical studies and experiments on single beams with different types of bracing have been completed, which have established the effect of brace stiffness on the lateral buckling strength (Yura and Phillips, 1992). Other phases are the evaluation of the stiffness characteristics of various types of bridge decks and a test on a full size multigirder bridge. The report herein presents the results of the full size bridge test. The purpose of the full size bridge test was to demonstrate the bracing effect of a bridge deck and to determine if a non-composite deck and steel beam can be treated as laterally restrained for load rating procedures. The study was done through a full scale test on a multi-girder 24-ft span bridge at the Ferguson Structural Engineering Laboratory, University of Texas.

It is well known that a steel beam without adequate lateral restraint of its compression flange may deflect and buckle laterally before the bending stress reaches yield stress. Hence, the stress at which buckling would occur must be determined to evaluate the beam's load carrying capacity. However, the capacity can be improved by bracing the beam along the span. In practice, beams are braced in a variety of ways. The slab, secondary stringer, or deck may act as a brace to the beams on which they are supported. Hence, in order to realistically and accurately determine the capacity of these beams, the effects of bracing must be considered.

Steel stringers are usually laterally or torsionally restrained either through the normal arrangement of the cross members in the framework or by diaphragms and diagonal bracing supplied as a precaution against buckling. These restraints have the effect of increasing the stability of the members, and in many cases it will be found that the beams will fail because of yielding under plane bending stresses before collapsing laterally. Thus, provided that the degree of restraint required to achieve stability may be determined, it will frequently be possible to design a slender beam on the basis of its material yield stress alone.

1.2 Scope of the Investigation

A full size bridge with a wood deck was tested to failure to demonstrate the strength of the bridge system. The bridge was comprised of five 24-ft-long S6x12.5 steel beams which supported a deck of 4x8 wood planks. There was no positive connection between the deck and the beams; the deck rested on the beams directly. The bridge was loaded through a standard truck axle and trailer filled with concrete blocks. Figure 1.3 shows a sketch of the bridge.

Preliminary tests were conducted to investigate the amount of bracing a single wood plank could provide to the steel beams. The single mode lateral buckling capacity and the plastic capacity of the beams were also determined.

From the above tests, the bracing effect of the wood deck is qualitatively and quantitatively assessed. Design guidelines are based on the current experimental work and on the tests conducted on the twin beams which formed the earlier phase of this project.

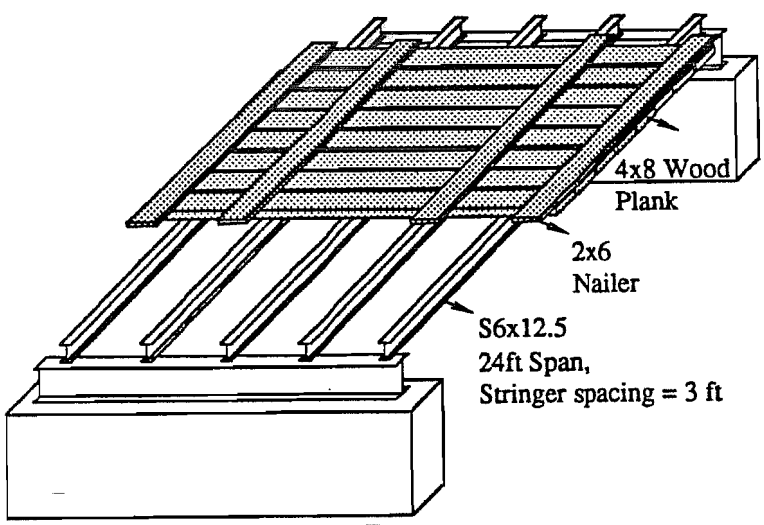

Figure 1.3 Sketch of the Bridge

1.3 Previous Work

The evaluation of the bracing effect of a bridge deck in contact with the steel stringers is usually related to the friction that may be mobilized at the deck-beam interface. Full scale laboratory and field tests were performed as a part of a research study completed by the New York State Department of Transportation (Kissane). The objective was to

determine if a non-composite concrete slab and steel beam could be treated as laterally restrained for load rating purposes. In the laboratory tests, a 21 ft long S12x31.8 beam was loaded to flange yield without indication of lateral stability. The research concluded that the friction mobilized provided the restraint. It is not clear, however, if this was the only restraint. The slab may also have prevented the top flange of the beams from twisting, thus providing torsional restraint. In the field test, the continuous slab acted as a load carrying member and the stringers supported only fifteen percent of the applied load. Since the beams carried less load than anticipated, they did not face any danger of lateral-torsional buckling. Thus, the field test did not give any real insight into the bracing effect provided by the deck. The full size test planned was aimed at studying the types of restraint provided by the deck and to see if it was sufficient to prevent lateral instability of the stringers.

A.R.Flint studied the stability of singe I-beams loaded through the top flange by secondary cross members resting on the beams at midspan. Based on analytical studies and experimental work on very small models, Flint concluded that no lateral buckling can occur in the first mode unless the beam has an initial bow greater than half the flange width. The secondary beams were propped cantilevers loaded with dead weight. Rollers, which were presumed frictionless, were placed between the main beam and the perpendicular secondary beam. However, it is doubtful that this system is friction free. Tests on twin parallel beams (Yura and Phillips, 1992) indicated that buckling can occur in the first mode contrary to the conclusions by Flint. Also, Flint's study did not consider the effect of cross-section distortion.

Chapter 2

THEORETICAL BACKGROUND

2.1 Theory

Structural members subject to transverse loads and moments acting in the plane of greatest stiffness may deform laterally and twist. This stability problem is well known as lateral torsional buckling and involves both an out-of-plane displacement and twist of the cross section, as shown in Figure 2.1. For an idealized perfectly straight elastic beam, there are no out-of-plane deformations until the applied moment reaches the critical value at which the beam buckles by deflecting laterally and twisting. These two deformations are interdependent; when the beam deflects laterally, the applied moment exerts a component torque about the deflected longitudinal axis which causes the beam to twist.

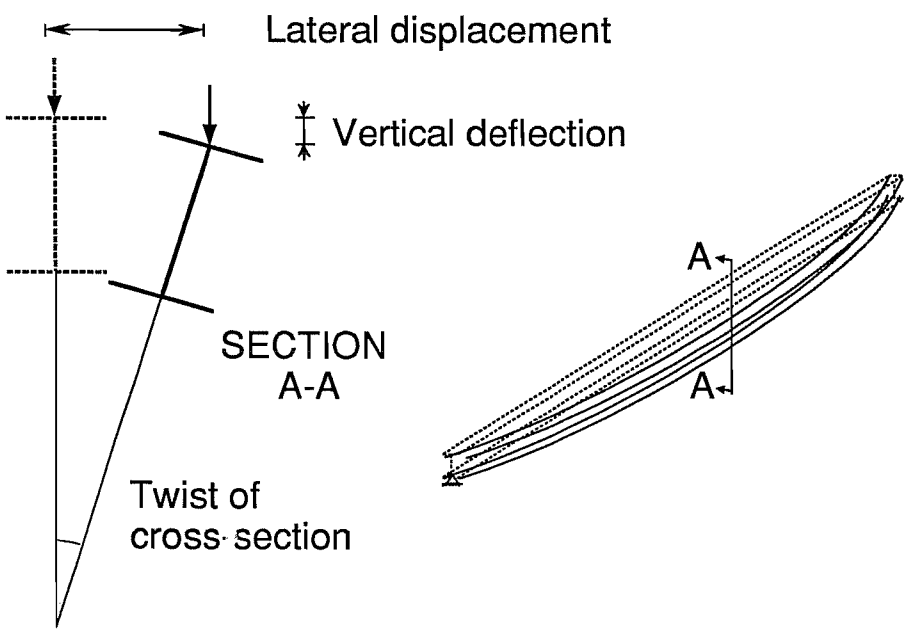

Figure 2.1 Lateral Torsional Buckling

The tendency of slender beams to buckle sideways, even though loaded solely in the vertical plane, may be greatly reduced by providing suitable bracing. An effective brace prevents the relative lateral movement of the two flanges. A simply supported beam is braced at a point if the compression flange is prevented from moving laterally. The point

is also considered braced if twist is prevented, say by a diaphragm between two parallel beams. In this case, both flanges must move laterally the same amount (no twist), so that point is a brace point. An ideal brace has the minimum stiffness required for the beam to buckle between braces. To do so, the brace must possess enough strength and stiffness. If the braces have less than ideal stiffness, the restraint may still be capable of increasing the buckling load sufficiently to induce yielding before buckling.

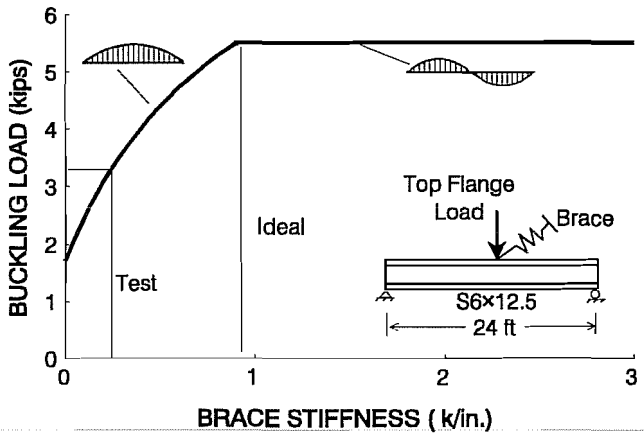

Figure 2.2 Beam capacity vs Brace stiffness

There are a number of ways in which a beam can be braced. The slab or deck which is supported by the beams in a bridge, secondary members through which a beam may be loaded, etc. can act as braces. These bracing members help in improving the capacity of the beams by providing, mainly, two types of restraints: lateral restraint and torsional restraint. As the name suggests, a lateral brace restrains the lateral movement of the beam, while a torsional brace restrains twist of the beam cross section. Figure 2.2 shows the relation between the beam buckling capacity and brace stiffness. An ideal brace forces the buckling to occur between the braces in a full sine curve (called second mode). For lesser brace stiffness, the beam buckles in a half sine curve (called first mode).

In the case of a deck resting on steel stringers, there can be restraint from different

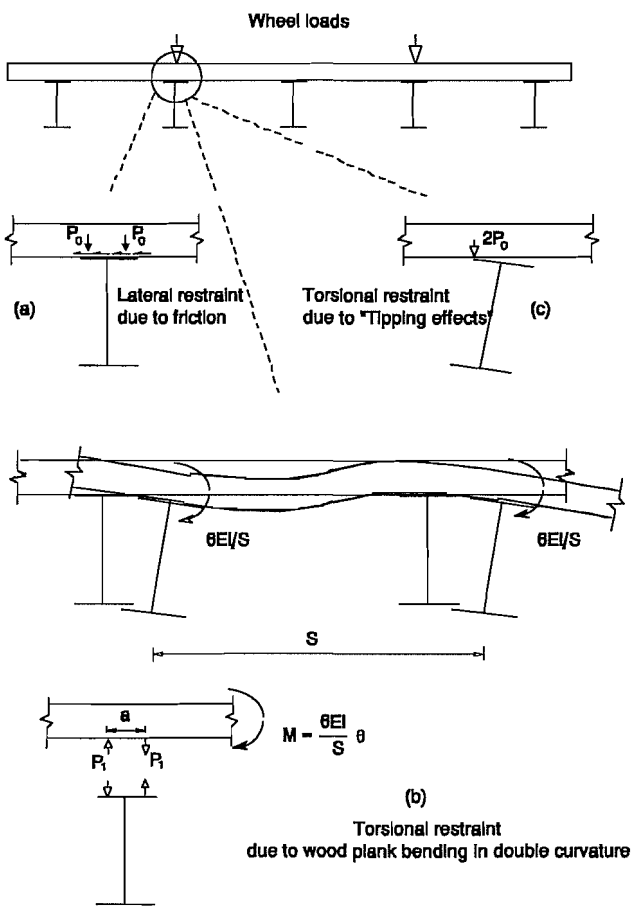

Figure 2.3 Restraint from Deck

sources. The friction that may be mobilized at the deck beam interface acts as a lateral brace, since it restrains lateral movement of the top flange, as shown in Figure 2.3(a). As the beam tries to twist during buckling, the deck planks provide torsional restraint in two ways. For the plank supporting the wheel loads there are contact forces P_o on the beam, as shown in Figure 2.3(b). There can be a restraining moment $M = 6EI\theta/S$ provided by the deck even when there is no positive attachment between the deck and steel stringer. In such cases M will produce contact force P_1 given by the relationship $P_1 a = 6EI\theta/S$ which is valid if $P_1 < P_o$. When the angle θ gets sufficiently large so $P_1 = P_o$, one side of the flange will separate from the wood plank and the restraint provided by the wood deck (6EI/S) goes to zero. However, at this stage the force on the other flange tip is $2P_o$ which provides a beneficial restoring torque for lateral stability called a "tipping effect." In reality, the bracing may be a combination of lateral, torsional, and tipping restraint.

The effectiveness of a torsional brace is affected by the distortion of the web at the brace location. Analytical and experimental studies (Yura and Phillips, 1992) have shown that the effective stiffness provided by a brace is greatly reduced because of this phenomenon. This reduction can be overcome by attaching a stiffener at the brace location. Analytical studies have shown that the effects of cross section distortion on the effective stiffness of lateral bracing placed at the compression flange are minimal and can be neglected.

Taking into account the improved capacity provided by the brace and the effect of cross-section distortion, the design equations developed by Yura (1990), based on analytical and experimental studies, were used to calculate the theoretical buckling capacity of the beams used in the full size bridge. These equations are given in Appendix B of Yura and Phillips (1992). The effectiveness of lateral bracing is based on the assumption that there is no relative movement (slip) between the beam and the deck at the wheel load.

2.2 BASP Analysis

The computer program BASP, Buckling Analysis of Stiffened Plates, (Akay) provides a general capability for the buckling analysis of plates having stiffener elements placed symmetrically about the plate (I beams). This program has been used extensively for the lateral buckling of beams and columns. In these applications, the web represents the plate, while the flanges are treated as stiffener elements. The web is idealized by two-dimensional finite elements, while the flanges are idealized by one-dimensional elements. Various planar geometry, loadings, boundary conditions, and elastic restraints can be accurately represented. The program accounts for cross-section distortion.

BASP was used to model the S6x12.5 bridge beams. Boundary conditions were specified as a pin and roller at the two ends, as shown in Figure 2.4. Braces were input as elastic springs at the nodes. Load was input as a downward concentrated load at the top flange.

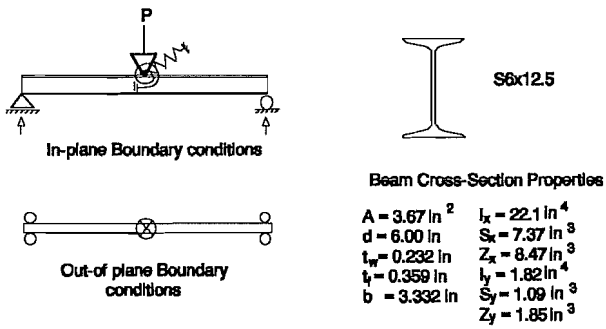

The single mode lateral-torsional buckling capacity was determined for concentrated load at the top flange at midspan, without any bracing. Assuming a certain stiffness for a lateral brace and torsional brace at midspan, the capacity of the beam with bracing was calculated. The second mode buckling capacity was determined by specifying a very stiff brace at midspan.

Figure 2.4 Analytical Model for BASP

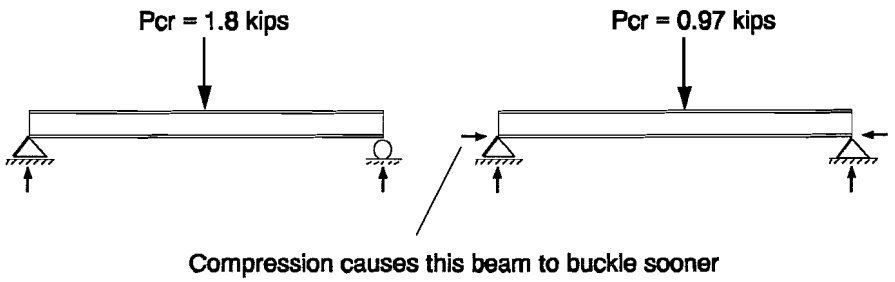

Figure 2.5 Effect of Axial Restraint

The effect of axial restraint at the ends on the buckling capacity of the beams was also examined. BASP runs were done for the bridge beam with pin-roller support conditions and pin-pin support conditions, as shown in Figure 2.5. It was found that the buckling capacity of a beam with pin-roller supports was almost twice the capacity of a beam with pin-pin supports. This is due to the detrimental effect of the compression that is caused when the supports are immovable. In reality, supports are not perfectly fixed and do provide flexibility. A typical end support in short span bridges is one in which the bottom flange of the beam is bolted down to supports.

In this report, BASP was used to compare with the various experiments and provide some indication of the significance of the various factors such as brace stiffness, end restraint, and so forth.

2.3 AASHTO Bridge Specification

Prior to 1989, the American Association of State Highway and Transportation Officials, AASHTO, recommended that beam buckling be treated as inelastic column buckling and that the following equation be utilized in Load Factor Design:

$$M_u = F_y S_x \left[1 - \frac{3F_y}{4\pi^2 E} \left[\frac{L_b}{b'} \right]^2 \right] \quad (1)$$

where M_u = lateral torsional buckling moment; F_y = yield stress of the material; S_x = major axis section modulus; L_b = unbraced length; and b' = flange width/2. The allowable moment in unbraced beams at service load in the AASHTO Bridge Specification, hereafter referred to as just AASHTO, was based on Equation (1) with a factor of safety of 1.8 which limits the maximum allowable moment to 0.55 $F_y S_x$.

In the 1990 Interim AASHTO, a more accurate and less conservative equation was presented for the determination of beam buckling strength,

$$M_u = 91 \times 10^3 C_b \frac{I_{yc}}{L_b} \sqrt{0.772 \frac{J}{I_{yc}} + 9.87 \left(\frac{d}{L_b} \right)^2} < M_y \quad (2)$$

where I_{yc} = weak axis moment of inertia of compression flange, J = torsional constant = $(2bt^3 + dw^3)/3$, d = depth of beam, t = flange thickness, w = web thickness, and M_y = yield moment. C_b is a modification factor for the moment diagram within the unbraced length. For an unbraced beam with a concentrated load at midspan, AASHTO recommends C_b = 1 but does permit C_b = 1.35 given in the SSRC Guide.

Equation (2) gives results very close to the Timoshenko classical lateral buckling formula (Timoshenko, 1960). Figure 2.6 shows values of beam buckling strength given by the 1983 and 1990 AASHTO specifications for a S6x12.5 beam with F_y = 42 ksi. As can be seen from the graph, the 1983 AASHTO buckling formula gives very conservative estimates of strength. In cases where the unbraced length is greater than 13 feet, the formula gives negative capacities. For example, for an unbraced length of 13 feet, the 1983 formula gives 0 k-ft, whereas the 1990 formula with C_b = 1.35 gives 20.74 k-ft.(M_y = 25.8 k-ft)

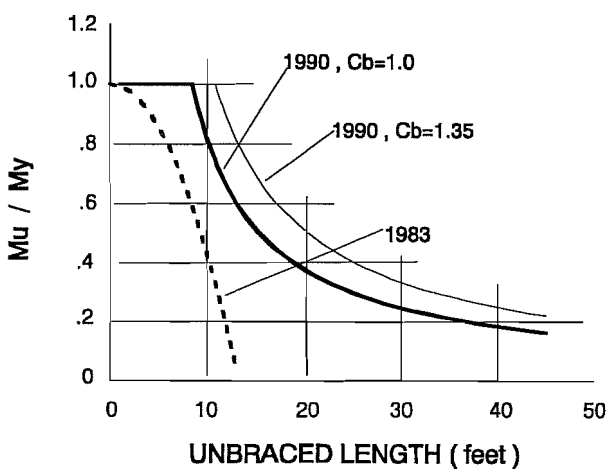

Figure 2.6 AASHTO Beam Buckling Strengths.

To counteract the unrealistic predictions given by the AASHTO Specifications prior to 1990, it has been common practice to assume that the truck wheel at midspan, which is the controlling loading condition for short span bridges, provides lateral support at that point. If this assumption is made in the previous example, the unbraced length would be

assumed as 6.5 ft and the 1983 AASHTO formula would give a buckling moment Mu = 19.6 k-ft, a very significant increase from the no-brace case. The principal purpose of the current research program is to determine if the truck wheel at midspan can, in fact, provide lateral support.

2.4 Texas Bridge Load Rating Program

The Texas bridge load rating program calculates load ratings in accordance with the AASHTO Manual for Maintenance Inspection of Bridges, 1983, and the AASHTO Standard Specifications for Highway Bridges, 13th edition, 1983. The purpose of the program is to simplify the load rating of non-standard bridges that are commonly found on rural roads off the state and federal highway systems.

In calculating the Inventory and Operating Ratings, the program uses the following basic equation of load rating.

$$\text{Inventory H-Rating} = \text{H15}\left\{\frac{(\text{Allowable Load} - \text{Dead Load})}{\text{LL (H15 vehicle)}}\right\}$$

The Basic equation expresses the load rating of the steel stringer as a ratio of the standard AASHTO H15 vehicle. The following describes the detailed steps involved in establishing a rating by the allowable stress design method.

1. The allowable load on the member is calculated at the inventory stress level. The allowable bending stress, F_b, is given by the formula,

$$F_b = A - B\left[\frac{L_b}{b}\right]^2 \qquad (3)$$

where A and B are shown in Table 2.1 with A = 0.55 F_y, the allowable bending stress for laterally supported beams; and B = $3AF_y / \pi^2E$.

2. The member load due to dead load is calculated.

3. The member load due to the H15 vehicle is calculated using the moment tables and the distribution factors which are related to the girder spacing and type of deck (AASHTO Bridge Specification, Section 3.23.2).

4. The inventory rating is calculated using the basic equation.

Table 2.1 Values of A and B

Yield Strength (ksi)	Allowable Bending Stress (ksi) A	Bracing Factor (ksi) B
26.0	14.0	0.0039
30.0	16.0	0.0052
33.0	18.0	0.0063
36.0	20.0	0.0075
45.0	24.0	0.0117
50.0	27.0	0.0144
55.0	30 0	0.0174

5. The operating rating is calculated using the basic equation with the allowable load on the member increased by the ratio of the operating to inventory allowable stresses.

By inputting the section properties of the bridge members and the dimensions of the bridge, the program calculates the load rating using the basic equation. The Rating Manual makes the following assumptions regarding the unbraced length to be used in the calculation of allowable bending stresses.

"A stringer is continuously braced (unbraced length = 0) if it is embedded in concrete. For stringers having a depth of 15 in. or less, a concrete deck or heavy surfacing may be assumed to provide continuous bracing by dead weight alone. This assumption should not be made if the bridge carries high speed traffic that might cause excessive vibration.

In other cases, the unbraced length is the distance between points where the top flange is supported laterally. In the absence of lateral bracing, reasonable ratings may be obtained by assuming an unbraced length equal to half of the span length. This assumption, which relies on friction from the wheel load, should not be made if the bridge carries high speed traffic that might cause excessive vibration."

Using this program to calculate the capacity of the bridge being tested led to an allowable stress of -53.1 ksi which would be taken as zero capacity. The calculations are shown in detail in Chapter 4 under Section 4.3.2.1. The unrealistic estimate is due to:

1. use of the conservative formula for beam buckling strength in the 1983 AASHTO; and

2. assuming no bracing from the deck.

PAGE

12

IS BLANK

Chapter 3

EXPERIMENTAL PROGRAM

3.1 General

The experimental program involved the design, construction, and testing of a full-scale 24-ft span multi-girder bridge with a wood deck. The bridge was load tested with a moving wheel load until failure. The bridge was comprised of five S6x12.5 steel stringers and a wood deck. The steel stringers, spaced at 3 ft, were bolted to W12x30 steel supporting beams at the two ends. The treated southern pine (wolmanized) wood deck was made of thirty-five 4x8 planks 16 ft long and was nailed to four 2x6 nailers. The middle two nailers also served as a guide for the cart. The details of the test setup are shown in Figure 3.1. The deck rested on the beams directly and there was no positive connection between the deck and the beams.

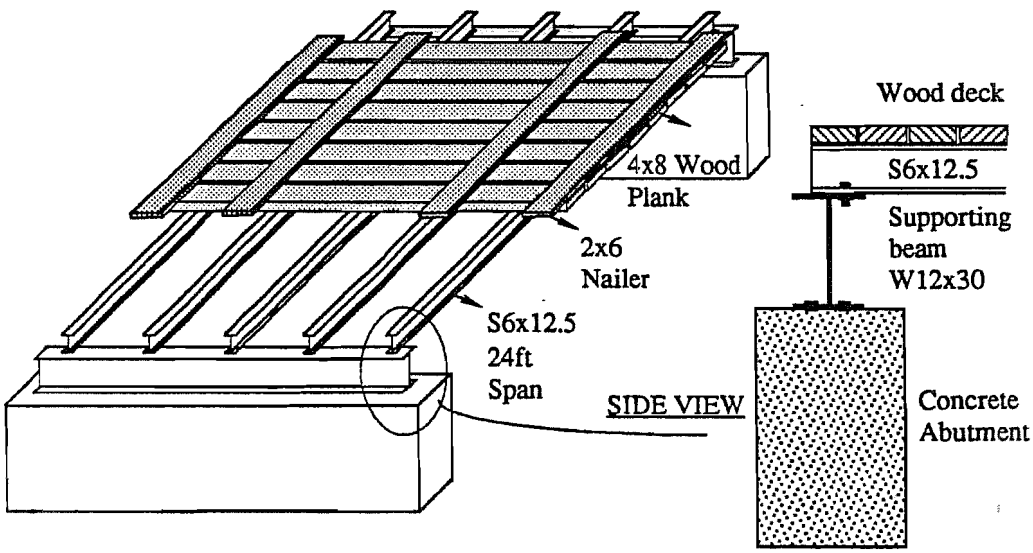

Figure 3.1 Details of the test setup.

Figure 3.2 is a photograph showing the overall view of the Test bridge.

In order to test the worst possible case, the loading was through a standard tandem (two tires on each side of axle) truck axle and only one axle of the truck was on the bridge. The axle load at midspan would be the governing load condition.

Preliminary tests were conducted to study the lateral buckling behavior and plastic bending strength of an individual beam. A series of lateral stiffness tests were conducted to

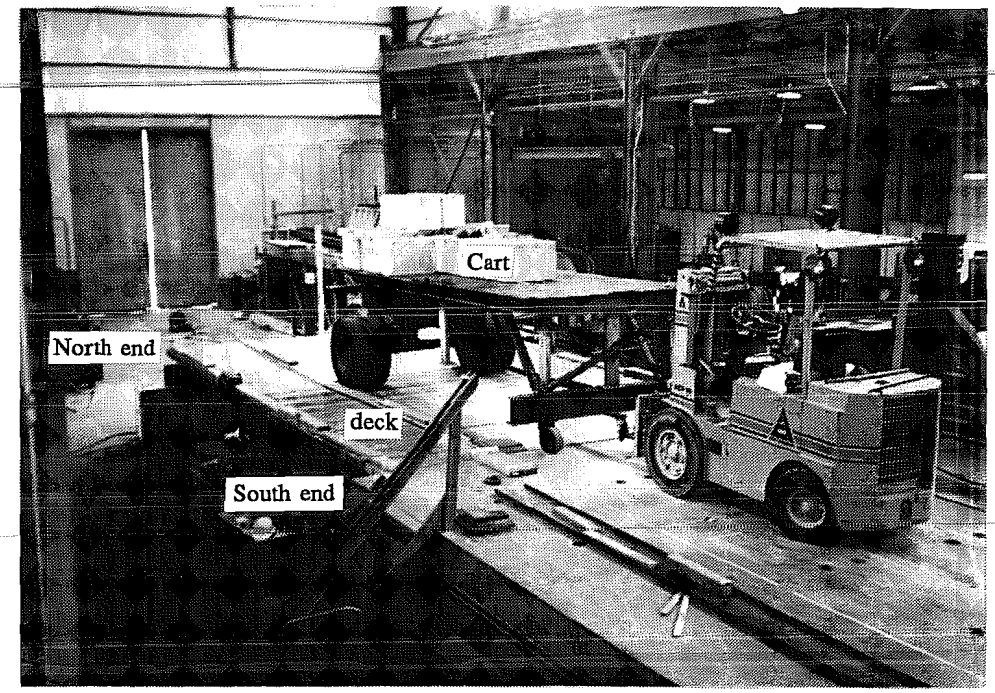

Figure 3.2 Photograph of experimental set-up.

evaluate the strength and stiffness of the deck and beams. These tests are described in detail in Section 3.6.

3.2 Design and Construction of the Bridge

The sections and span were chosen so that there was a significant difference between the single mode (unbraced) buckling capacity and the yield capacity of the stringers. This way, the bracing effect of the deck, if any, could be clearly demonstrated. The size of the beams was also limited by the magnitude of dead weight that could be safely used to load the bridge. A maximum load of 30,000 lbs on the cart to produce an axle load of 22,000 lbs was practically feasible in the laboratory. The end supports, beam spacing, and other details were based on conditions found on typical bridges in Texas. The size of the wood planks was controlled by the bending moment in the planks as the wheel loads are distributed to the five stringers.

The construction of the bridge involved assembly of the steel stringers and bolting them to the end supports. The abutment was comprised of concrete blocks to which a W12x30 was bolted. The end detail is shown in Figure 3.1. The 4x8 wood planks were laid on the bridge with an approximate spacing of a quarter of an inch. The 2x6 planks were used as nailers to keep the planks aligned and also to serve as a guide for the cart. The nailers were spliced at the third points and were nailed to the planks with 3-in.-long steel screw nails spaced at 8 in. The wood deck was connected to an external support at the south end, through connecting beams, to prevent it from moving off the steel beams longitudinally, due to the braking action of the loading cart. The connection was designed to minimize any

in-plane restraint to the steel stringers. The details are shown in Figure 3.3. At the north end, lateral movement was prevented by nailing wood boards between the beams. All connections were designed for a lateral force of 1 kip. Connection details were made so that they did not provide any kind of extra restraint to the stringers.

3.3 Loading System

A steel cart measuring 16-ft x 12-ft and loaded with concrete blocks was used to load the bridge. The cart was fitted with a truck axle (tandem) on one end and rested on castors at the other. The center to center distance between the tires was 6 ft. Only the axle load was applied to the bridge, the castors remained on an elevated slab adjacent to the test bridge. A forklift was used to push the cart on and off the bridge. Figure 3.4 shows a photograph of the cart and the bridge.

At each stage of loading, the wheel load on each side of the axle was weighed and then slowly moved onto the bridge. The cart was used as a loading system instead of a hydraulic ram since it closely simulated a real vehicle in terms of tire contact area and load distribution. The moving wheel load also took into account any vibration that may be present when a vehicle moves over a bridge. One of the factors considered was the effect of vibration on the frictional restraint provided by the deck. However, the slow movement of the cart required by laboratory testing did not represent vibrations associated with actual truck loading. Vibrations may affect the frictional restraint provided by the deck. To overcome this deficiency, a concrete vibrator was attached to the deck. The cart was designed to carry a load of 30 kips, with the truck axle carrying 75% of the total load. Concrete blocks each weighing 400 lbs were arranged so that this load distribution was achieved. The load was increased in 0.6 - 1.4 kip increments.

3.4 Instrumentation

The instrumentation used in this experiment is shown in Figure 3.5. The various physical quantities measured were strains, displacements, relative movement, and twist of cross section. All gauges were monitored with a automatic data acquisition system coupled to a computer for data storage. This enabled readings to be taken every few seconds.

Strain gauges with gauge length of 8 in., installed following standard installation procedures, were used at two locations on the beams to give an estimate of the load carried by each beam. At each location, four gauges were placed on the web, as shown in Figure 3.5. The strain gauges were calibrated by dead weight testing of each beam to give an accurate indication of moment. A known point load was applied at the midspan of each beam and the strains were measured. Calibration curves between the applied moment and measured strains were developed. These were used to calculate the load from the strains measured during the actual test.

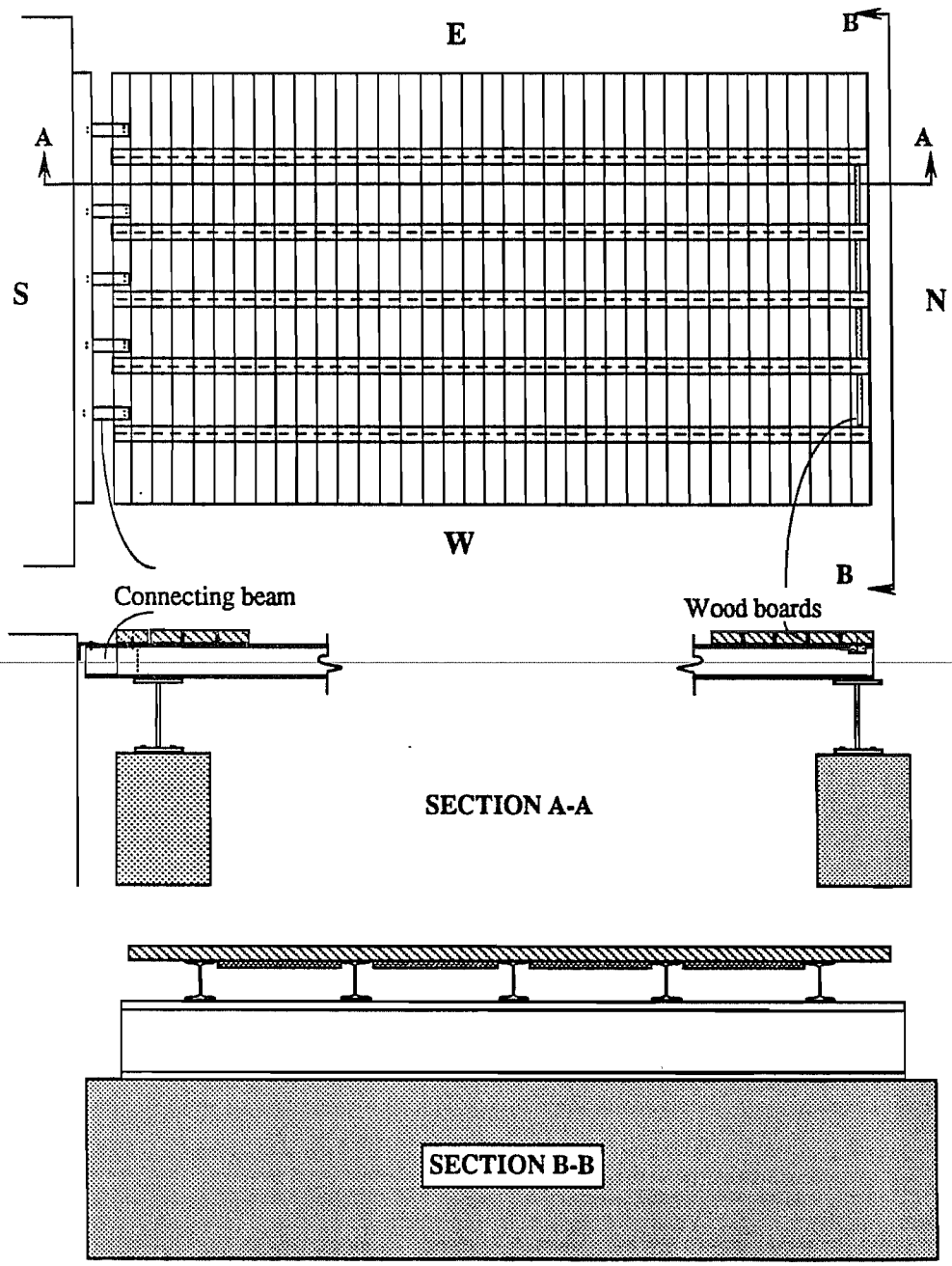

Figure 3.3 End connection details.

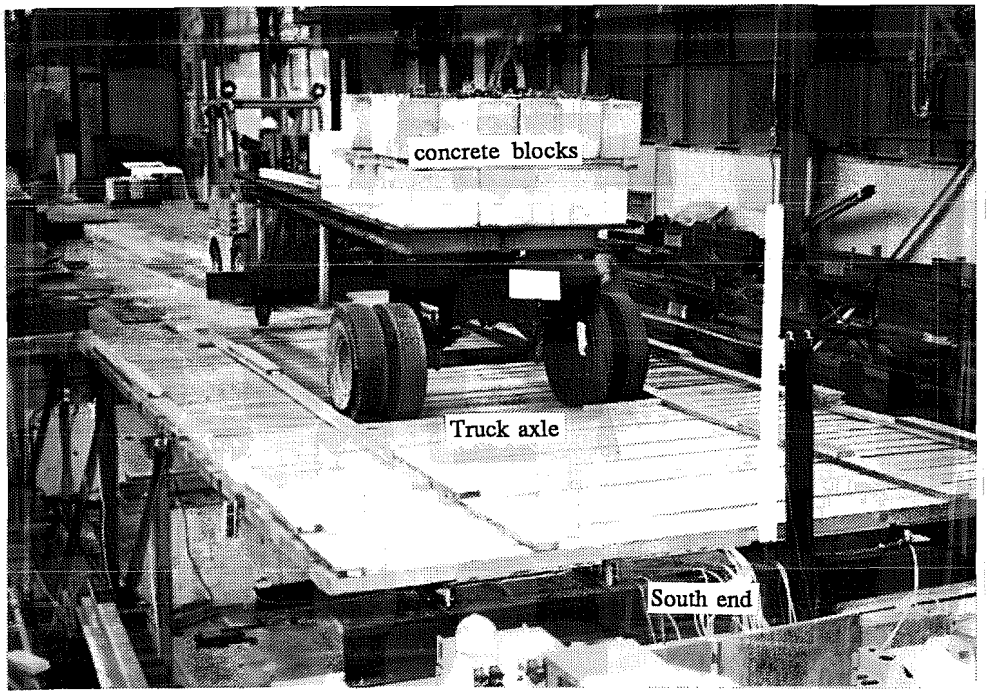

Figure 3.4 Photograph of the bridge and cart.

Linear potentiometers were used to measure the relative slip between the top flange of the beam and deck. Fifteen gauges were used to measure the relative movement at midspan and the quarter points on each of the five beams. Figure 3.6 shows the location of the gauge. Two linear potentiometers were installed to measure any sidesway of the bridge cross section at the two ends of the bridge.

Displacement transducers were used to measure the vertical deflection of the five beams at midspan. Three gauges were installed to measure the lateral movement of the deck at midspan and quarter points. A 400-in. stroke displacement transducer kept track of the position of the cart on the bridge.

At each stage of loading, the load coming on to the axle of the cart was measured using two 2000-lbs weighing scales. These portable scales are normally used to measure vehicle weights in the field. The scales were calibrated by applying known loads in a testing machine. The scales were accurate to within 100 lbs.

The central 8-ft portion of each beam was whitewashed as an aid to detect yielding.

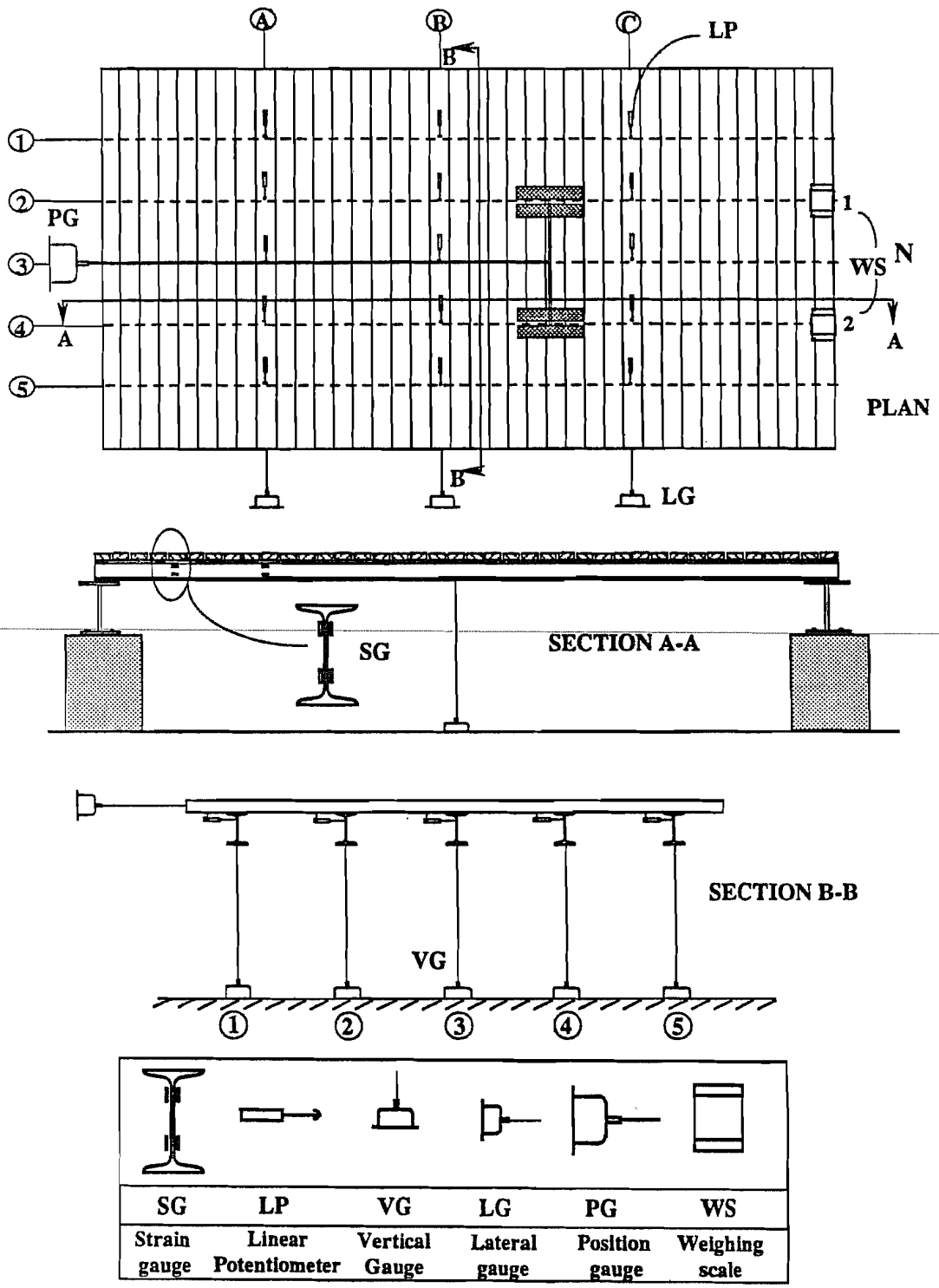

Figure 3.5 Schematic of instrumentation.

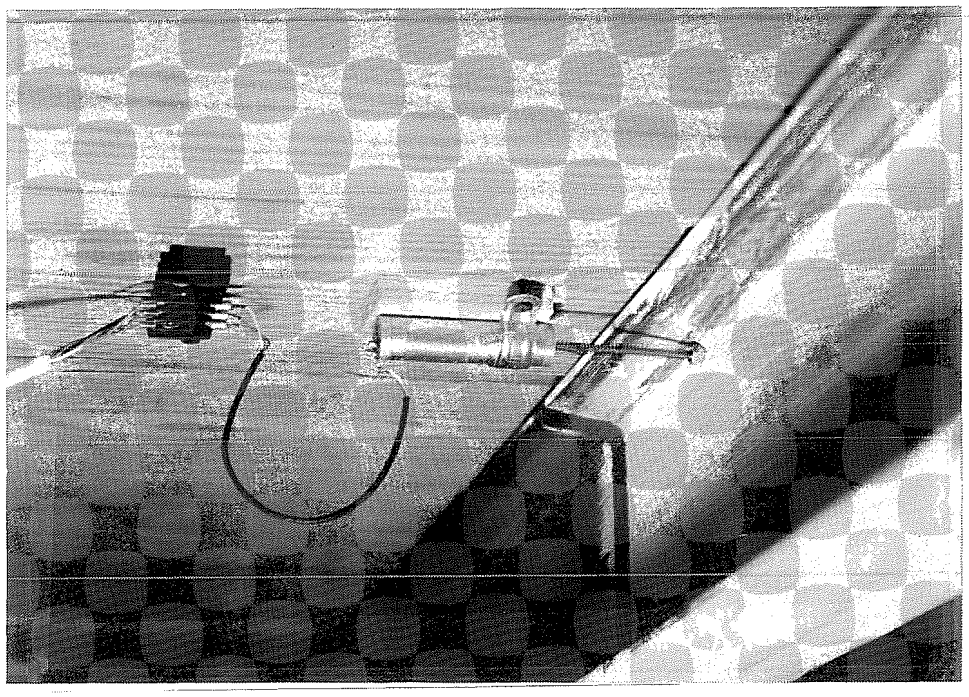

Figure 3.6 Photograph of gauge used to measure relative slip.

3.5 Material Tests

The five steel beams were chosen from the same mill batch to ensure uniformity in beam properties. Coupon tests were done on a representative beam. Standard coupons with an 8-inch gauge length were cut from the web (two coupons) and the flanges (two coupons) of the beam section and the static yield and ultimate capacity were determined. The static yield capacity was used in the estimation of the theoretical buckling capacity of the beams.

Table 3.1 Material Properties of Bridge Beam

Static Yield Strength (ksi)			Ultimate Strength (ksi)			Plastic Moment (Yield Moment)
Web	Flange	Average	Web	Flange	Average	355.3 k-in (309.5 k-in)
42.4	41.8	42.1	66.0	67.2	66.6	

The average values of the static yield and ultimate strength are given in Table 3.1.

The handbook cross-section properties of the bridge beam are shown in Figure 3.7. Measured properties are shown in parentheses. Since there is very little difference between handbook and measured properties, handbook properties will be used throughout this report.

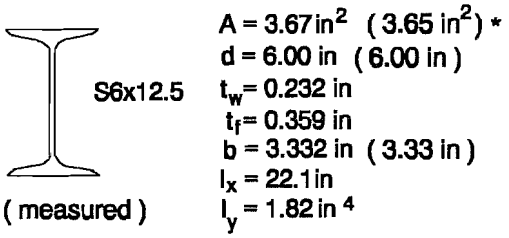

Figure 3.7 Cross-section properties of bridge beam.

3.6 Preliminary Tests

Various preliminary tests were done to gather information on the components of the bridge system.

One of the concerns was the effect of axial restraint on the buckling capacity of the beams. BASP was used to analyze the effect of pin-pin support versus pin-roller support. Two tests were conducted to study this experimentally. The end support details used are shown in Figure 3.8. The capacity in both cases was very close to the pin-roller case (as predicted by BASP). This can be explained by the fact that the web of the supporting beam bends and provides very little restraint in the x-direction. Hence, for the support arrangement used on the bridge, the support conditions approximate a pin-roller support. Figure 3.9 shows the end support condition for the bridge beams.

To get an estimate of the single mode lateral torsional buckling capacity of the bridge, a S6x12.5 beam, 24-ft span was tested with a concentrated load on the top flange at midspan, as shown in Figure 3.10. The load was applied through knife edges. A photograph of the test setup is shown in Figure 3.10. A schematic of the tests is shown in Figure 3.11. Two beams were used so as to make use of an already existing test setup from the earlier phase of this project. Details of the test setup are given elsewhere (Yura and Phillips, 1992). A second test was done, with the load applied through a steel tube resting on wood pieces at midspan. The wood pieces just rested on the top flange of the beams; no positive attachment was provided. This was done to study the "tipping effect" and is similar to the load transfer from the deck to the bridge beams. However, the wood pieces were in full contact with the top flange, which was not true in the case of the test bridge. The plastic moment capacity of the beam was also determined by bracing the stringer along the span; the capacity of 360 k-in. corresponding to 5.0 kip test load was close to the plastic capacity calculated from the coupons as shown in Table 3.1. This gave an upper limit to the bridge capacity. These results are summarized in Table 3.2. Placing a single plank at midspan with no positive attachment increased the buckling load from 1.7 kips to 3.6 kips. In both cases, the buckled shape was a single mode shape, so the plank did not act as an ideal brace. If the beam was completely braced at midspan, the expected capacity would be 5.5 kips, which means the beam would yield at midspan before buckling could occur. The load vs lateral deflection curves are shown in Figure 3.12. The load vs vertical deflection curve for the plastic moment test is shown in Figure 3.13.

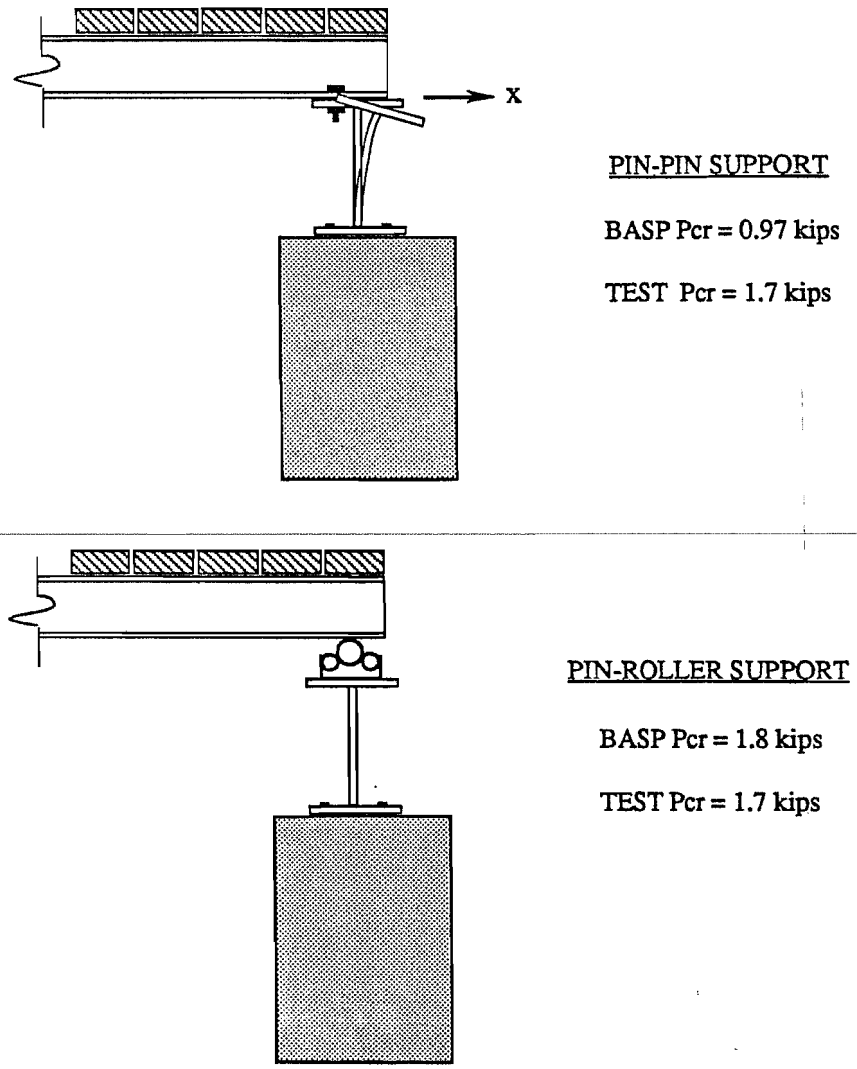

Figure 3.8 Tests to study end axial restraint.

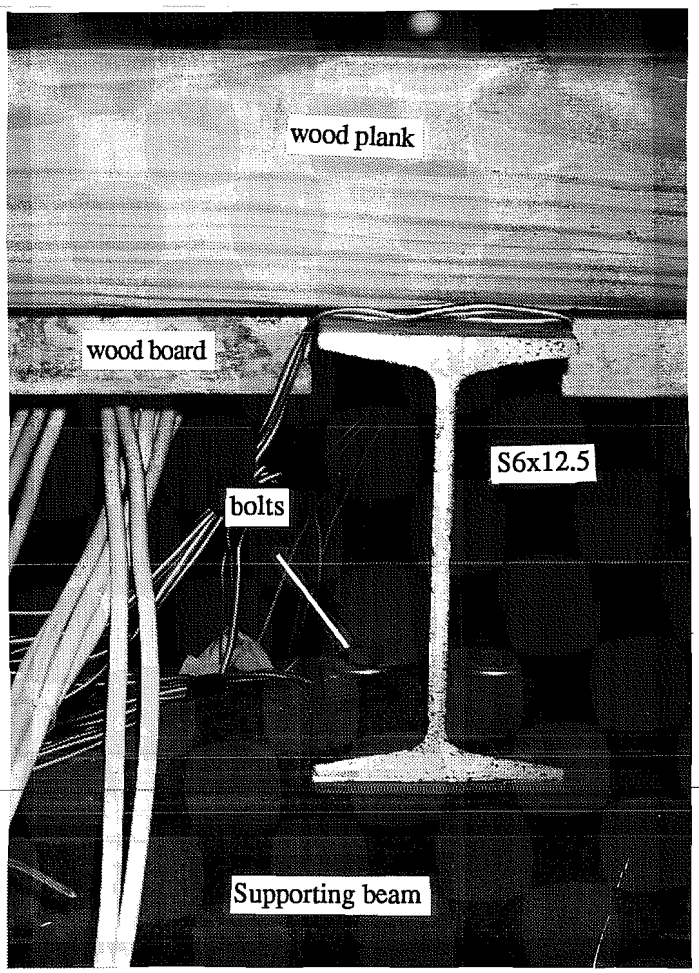

Figure 3.9 Photograph of end support detail.

Table 3.2 Summary of Preliminary Tests

Mode of Failure	Single Beam Capacity (kips)
First mode LTB	1.7
Tipping effects	3.6
Plastic capacity	5.0

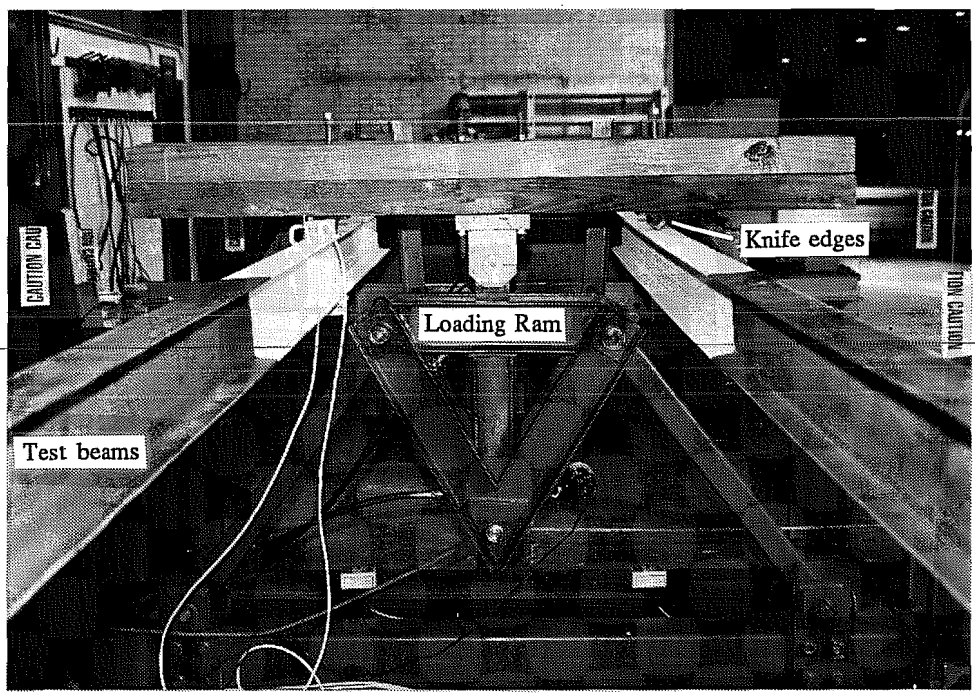

Figure 3.10 Test setup for first mode LTB test.

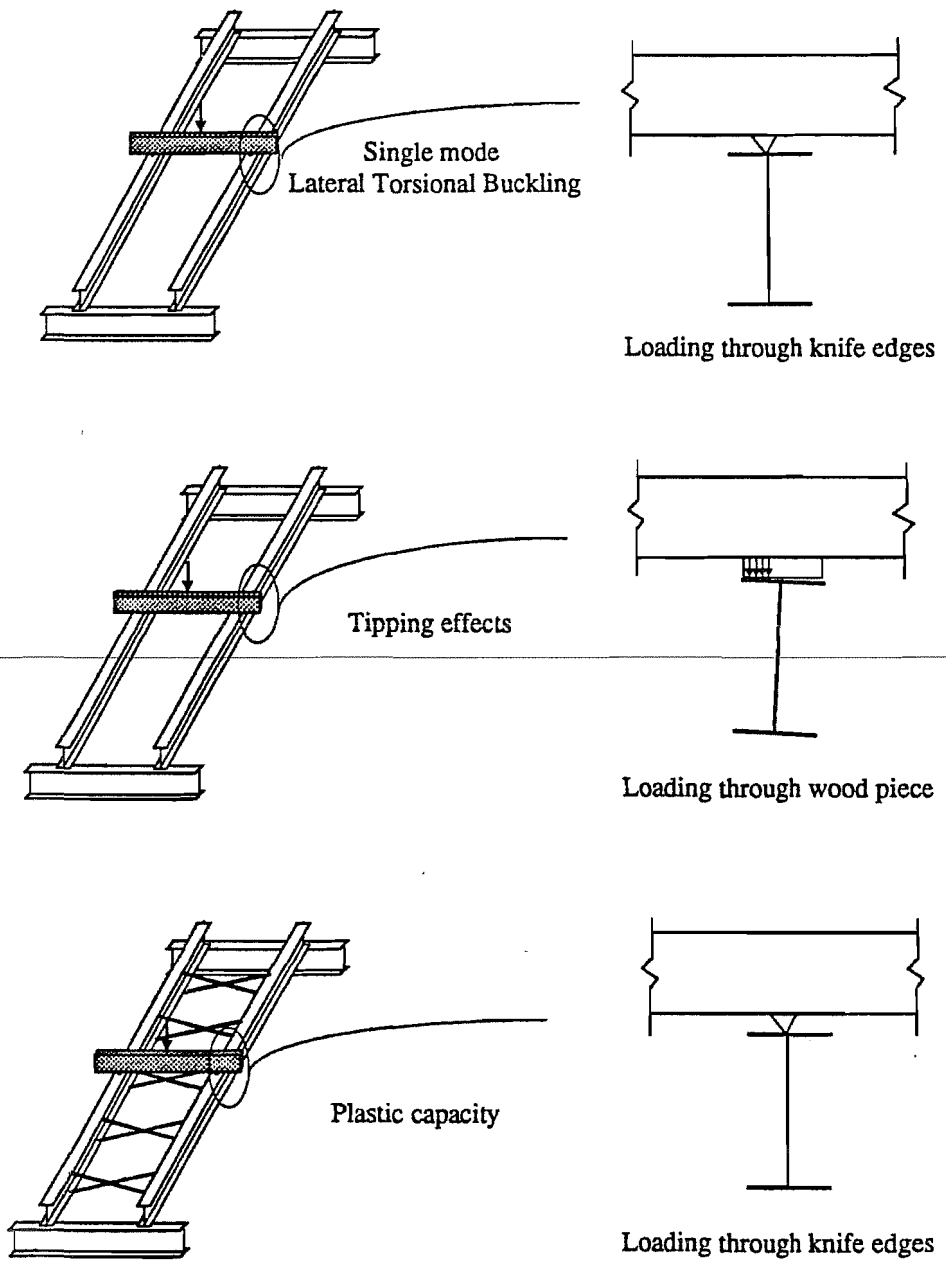

Figure 3.11 Schematic of preliminary tests.

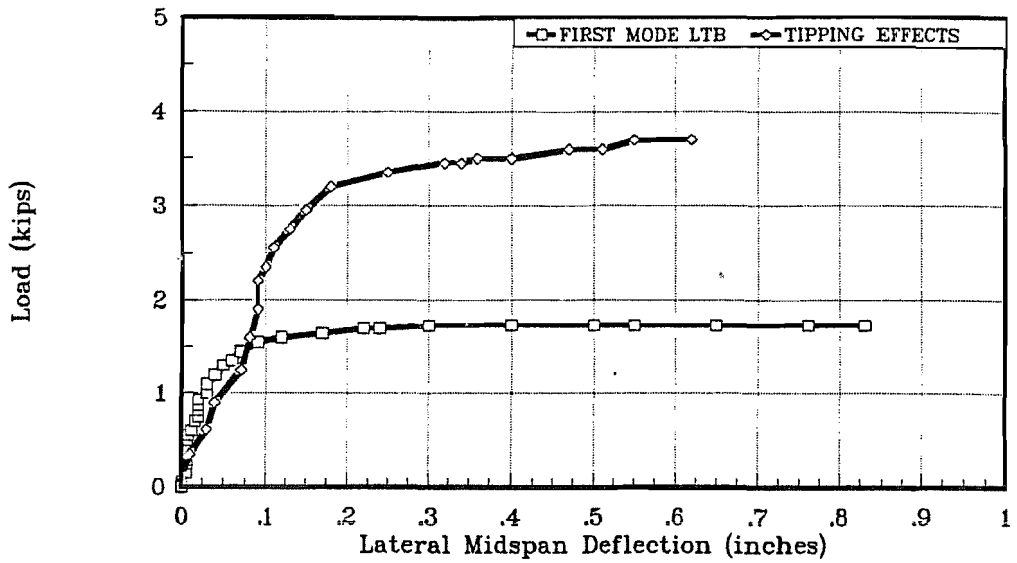

Figure 3.12 Lateral buckling curves.

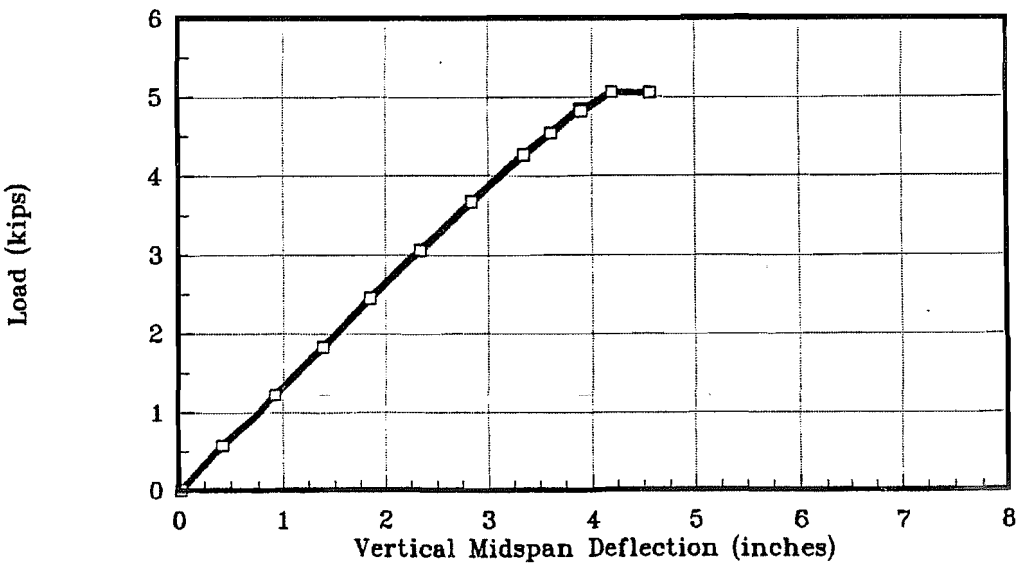

Figure 3.13 Load deflection curve for plastic capacity test.

Pg. 26

Blank
page

Chapter 4
TEST RESULTS

4.1 Test Procedure

The bridge was loaded with a cart filled with increasing weights of concrete blocks until failure. Failure was defined as significant lateral movement of beams and deck or yielding of beams. The first loading level was with the dead weight of the cart, which measured 3.5 kips at the axle. A forklift was used to push and pull the cart. At the beginning of every run, the cart was positioned so that the tires rested on the weighing scales. The scales were read and a scan of all the gauges was made. The cart was then slowly pushed on to the bridge until the wheels reached midspan and then the cart was pulled off the bridge. Readings were taken every few seconds. The cart was stopped at the quarter point and midspan so that the bridge could be examined, photographs taken, and static data recorded. No quarter point static data were recorded when the cart was pulled off the bridge. For each stage of loading, three runs were done. The first and third runs were done without the vibrator, while the second run was done with the vibrator. The loads were increased by adding concrete blocks, the increments being in the 0.6 - 1.4 kip range.

At the midspan of each beam, the edge of the top flange was marked directly on the wood deck to monitor their relative movement. A video camera recorded any movement of the beams as the cart moved over the bridge. Close attention was paid to the behavior of the wood planks as the wheels moved over them. Visual inspection of the whitewashed portion of the beams was made to check for yield lines.

4.2 Presentation of Test Results

The strains, vertical displacements, lateral displacements, and reactions due to the applied increments of load are presented in tabular form in Appendix A. The following sections describe the procedure adopted to process the collected data.

4.2.1 Data Selection. As a first step, the three runs made at each load level were examined for any significant differences in the measurements made. Strain gauge readings, vertical gauge readings, and lateral gauge readings were compared for the three runs. The comparison was also made at different load levels. It was observed that there was no significant difference in the gauge readings for the three runs except in the final load stage, which was the load at which the bridge failed. Hence, only the data collected for the third run at each load level were used for the analysis. For the last load level, only two runs were completed before the bridge failed and both were used for data analysis.

4.2.2 Load Calculations. The load carried by each beam was calculated from two sources, the strain gauge readings and the vertical gauge readings.

Strain gauge readings. The strains were measured at two locations on each beam, as shown in Figure 4.1. The load on each beam was calculated by relating the bending

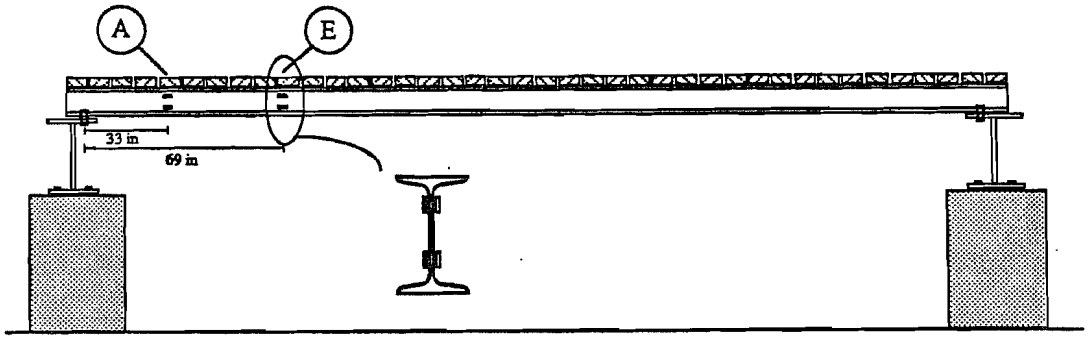

Figure 4.1 Strain gauge location.

moment at the section at which the strains were measured to the strain gauge readings. The relation between bending moment and strains was determined from strain gauge calibration tests. This is a function of the geometric and material properties of the cross section. Since there could be inaccuracies in assumed values, the calibration tests give a more accurate measure of the actual beam characteristics. For a known position of the cart, the load in each beam was determined from the measured bending moment. These calculations were done for the two sets of strain gauges on each beam, as shown in Figure 4.1, at A and E. The average percent difference was found to be 5%. From previous tests, in which known loads were applied and strains were measured, it was observed that strain gauges at E gave more accurate correlation with the applied loads. Hence, these load calculations are used in all subsequent calculations and discussions.

Vertical gauge readings. The vertical displacements of the five beams were measured at midspan using displacement transducers. Though the strain gauges were primarily meant for load calculations, the vertical deflections were used as a second source. The vertical displacements at midspan were related to the bending moment on the beams using the conjugate beam method. The relation is a function of beam material and geometric properties and boundary conditions. From the bending moment, the load was determined for a known position of the cart. The calculations assumed idealized pin-pin support conditions, though this is not fully true. Hence, the absolute values of the loads determined were not used, but they were useful in determining the relative magnitude of the loads distributed among the five beams.

From the strain gauge and vertical gauge load calculations, which were within 4% of each other, the strain gauge calculations were used. From an earlier test in which gauge

readings were taken as the deck was placed, it was found that the strain gauge readings gave the closest correlation to the sum of the known weights of the planks used to form the deck. Hence, the strain gauge readings are used in subsequent sections as a source for load calculations.

4.2.3 Load vs Vertical Deflection Curves. The relation between the load and vertical displacement is a measure of the stiffness of the beam. The load deflection curves are plotted for the five beams and are presented in Figure 4.2. The load on the axle, that is, the live load coming onto the bridge, as measured by the weighing scales, is plotted on the y-axis, while the vertical deflection of each beam at midspan is plotted on the x-axis..

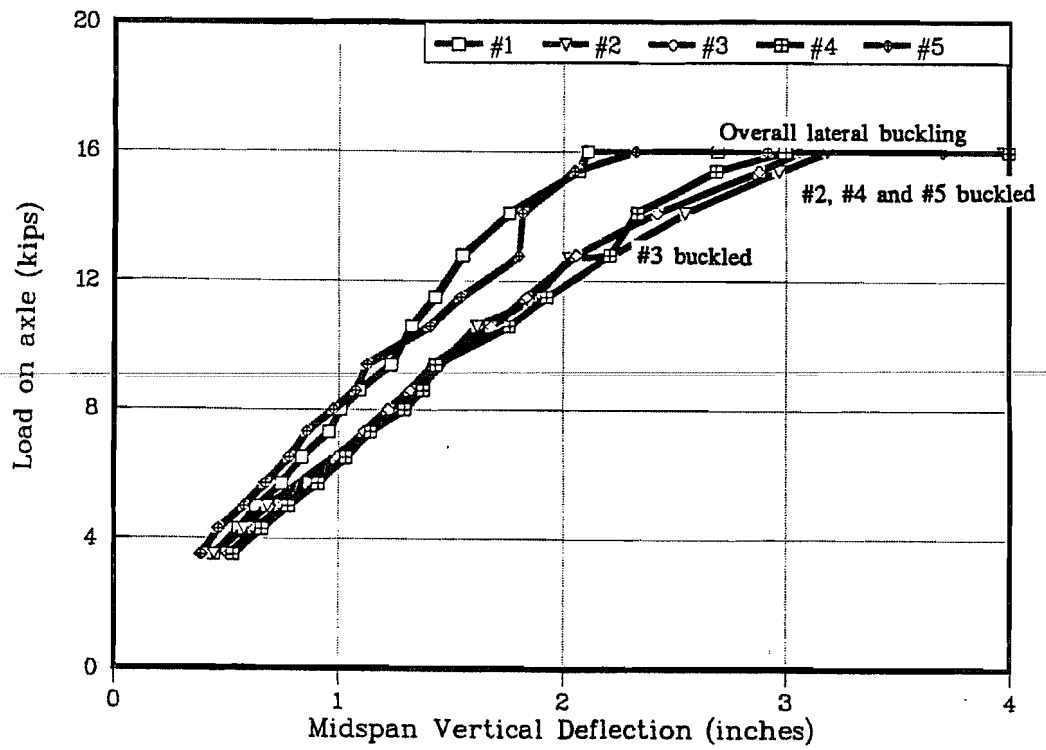

Figure 4.2 Load vs. vertical deflection curves for the five bridge beams.

As can be seen from the graph, the beams exhibit nearly linear elastic behavior up to a load of 14.1 kips for all beams except Beam #3. Beam #3 buckled first at a load of 12.8 kips. The curves flatten at 16.0 kips, indicating that there is change in behavior. This can be explained by the fact that at the ultimate load, the beams experienced lateral torsional buckling and lost in-plane stiffness. The three interior stringers showed very similar deflection behavior, indicating that they were supporting nearly equal loads. Similarly, the two exterior girders were similar to each other and they deflected less than the interior beams.

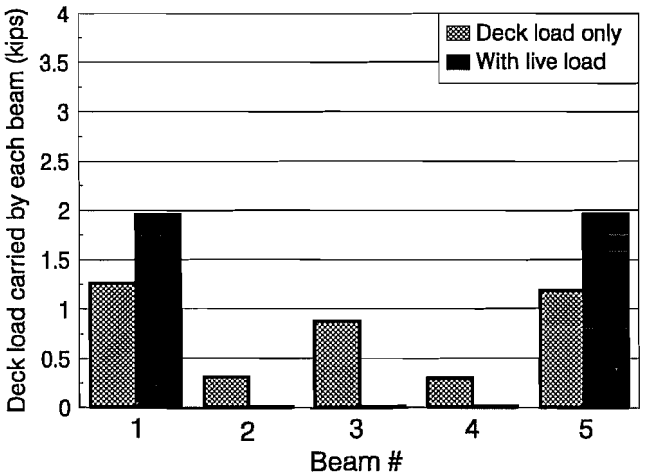

Figure 4.3 Distribution of deck load.

4.2.4 Load Distribution. The loads distributed to each beam were determined from the strain gauge readings. The load distribution is a function of the deck stiffness, beam stiffness, stringer spacing, and initial camber of the stringers and the wood planks. The weight of the deck was determined by measuring the strains before and after the deck was constructed. The distribution of the deck load is shown in Figure 4.3.

From visual observation it was noted that, as the wheel load moved on to the bridge, the three central beams picked up more truck load than the exterior beams and hence they deflected more than the exterior beams, thereby causing the deck itself to rest on the exterior beams. This caused the entire deck load to be transferred to beam #1 and beam #5, the exterior beams, except for the particular plank supporting the axle load. The planks did not touch the three interior beams at all, except for the one which was loaded. This plank was in contact with all five beams. Figure 4.3 shows the distribution of the deck load among the five beams before (deck load only) and after the cart comes on to the bridge (with live load). Initially, before the cart came onto the bridge, the two exterior and the center stringers picked up most of the deck load. After the cart came on to the bridge, the deck load was carried mainly by the exterior stringers.

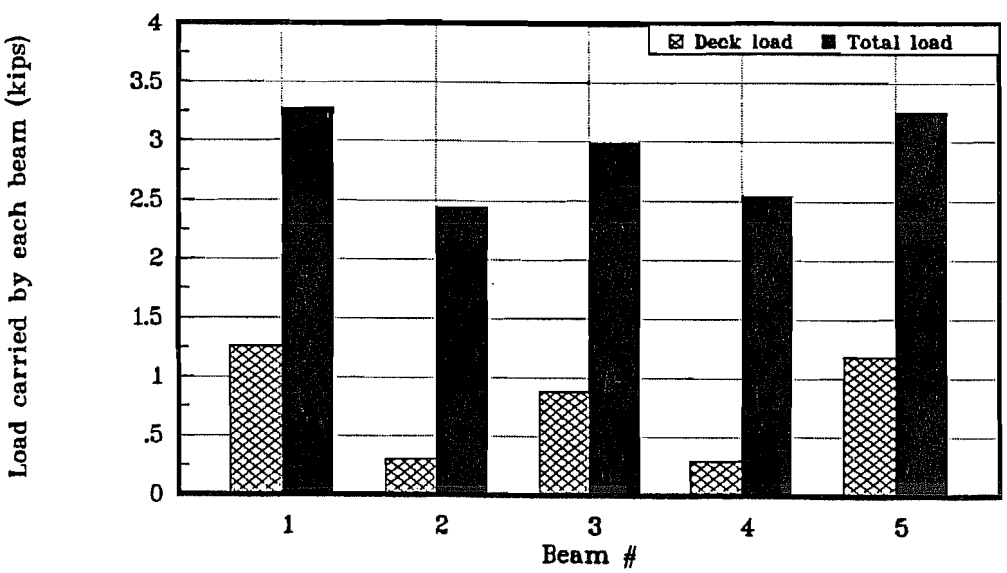

Figure 4.4 Total load distribution for an axle load of 10.6 kips.

For an axle load of 10.6 kips (includes weight of cart and concrete blocks coming on to axle), Figure 4.4 shows the total load distribution (deck load + live load). The total load is almost uniformly distributed among the five beams.

For an axle load of 10.6 kips, Figure 4.5 shows the live load distribution, calculated by subtracting the deck load distribution after the cart comes onto the bridge from the total

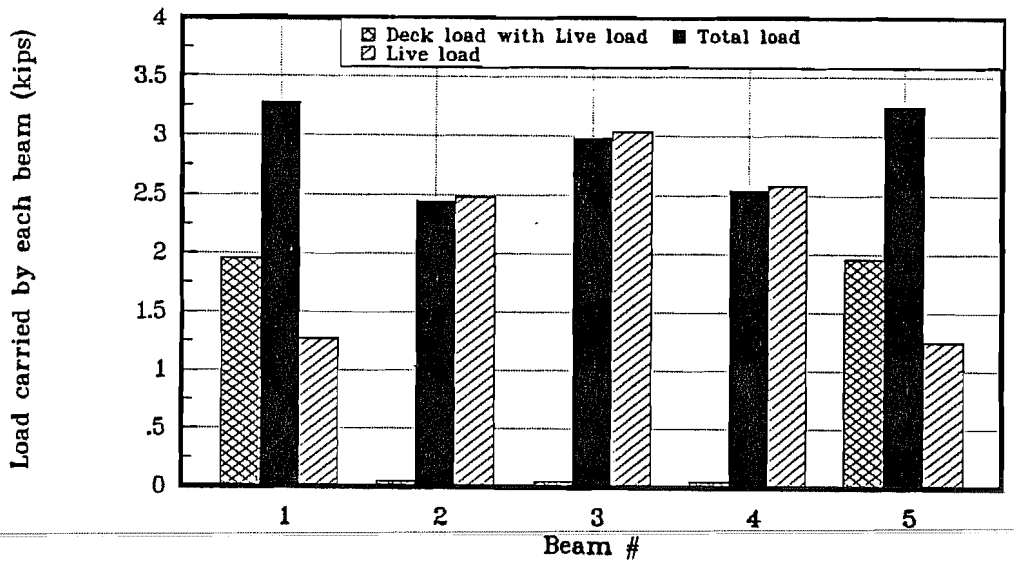

Figure 4.5 Live load distribution for an axle load of 10.6 kips

load distribution. From the above graphs, it can be seen that the central three beams pick up most of the live load, while the total load is picked up almost uniformly by all the five beams.

4.2.5 Load vs Lateral Deflection Curves. The lateral deflections of the beams were measured by linear potentiometers, while the lateral deck deflections were measured by displacement transducers. The displacements were monitored at three locations along the span; at midspan and the two quarter points. Figures 4.6 through 4.10 show the lateral deflection curves of the five beams. On each graph, the lateral displacements of the quarter points and midspan of each beam are plotted on the x-axis. The positive x-direction implies movement of the beams toward the east, as shown in Figure 3.2. Significant lateral movement of beam #3 was noticed after an axle load of 12.8 kips. Beam #3 was the first to start buckling in a single mode. Beams #1, #2, #4, and #5 remained nearly straight until a load of 14.1 kips. At lower load levels, the beams returned to their original straight position once the cart was off the bridge. The data points taken after a load level of 14.1 kips may not be accurate, since the linear potentiometers were bent during the test. This may explain the zigzag movement at quarter point on beam #3.

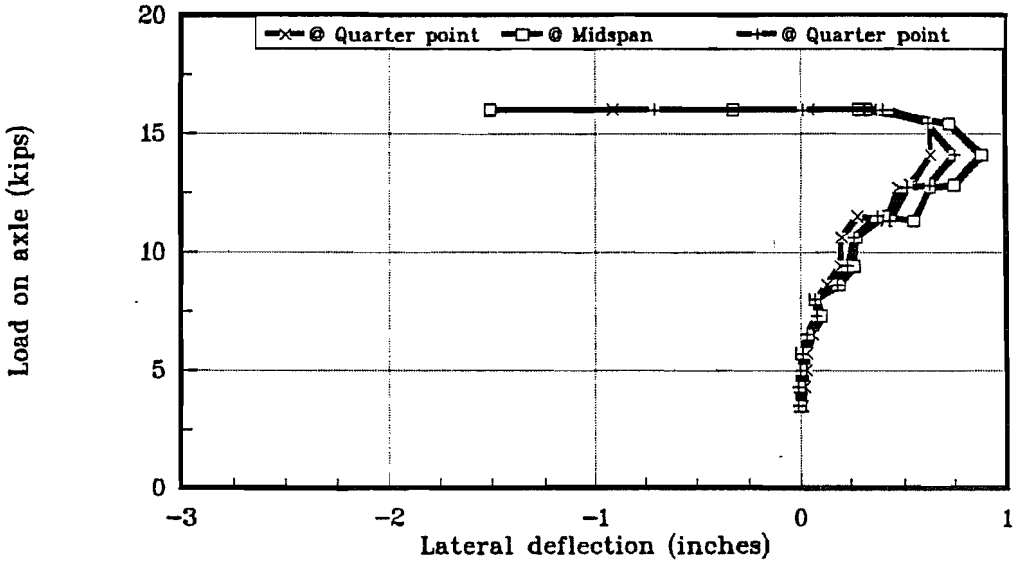

Figure 4.6 Lateral displacement curve for Beam #1.

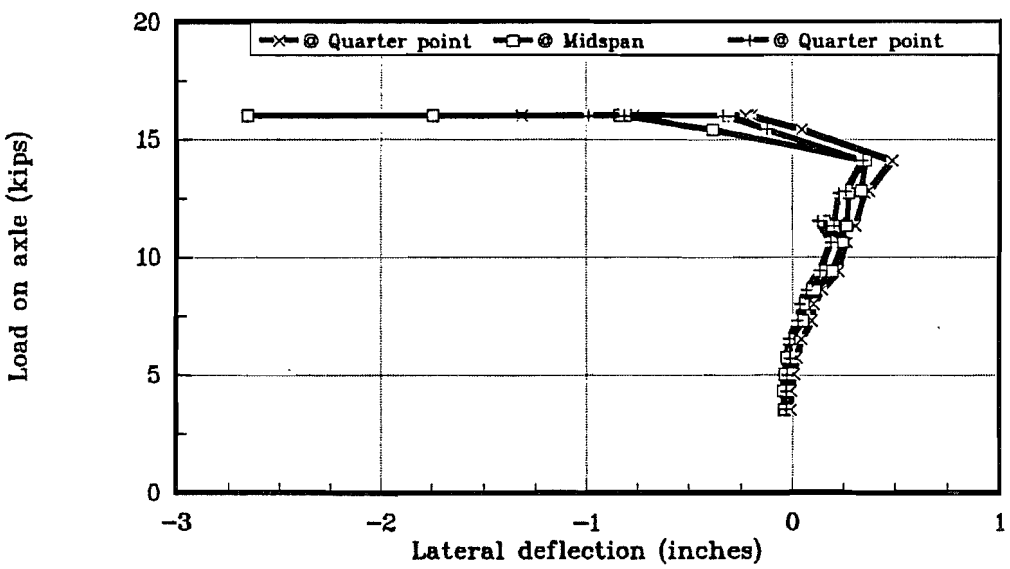

Figure 4.7 Lateral displacement curve for Beam #2.

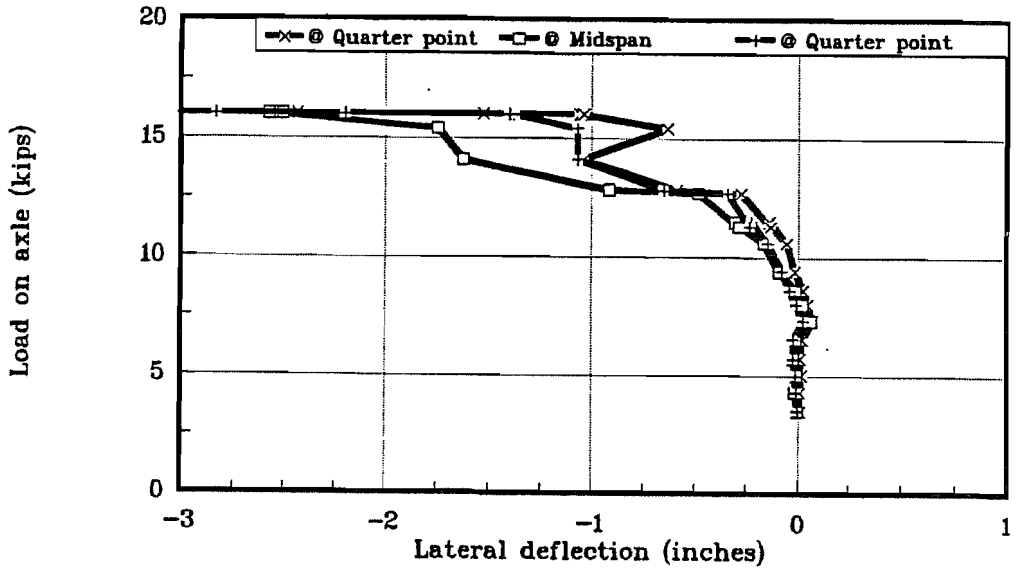

Figure 4.8 Lateral displacement curve for Beam #3.

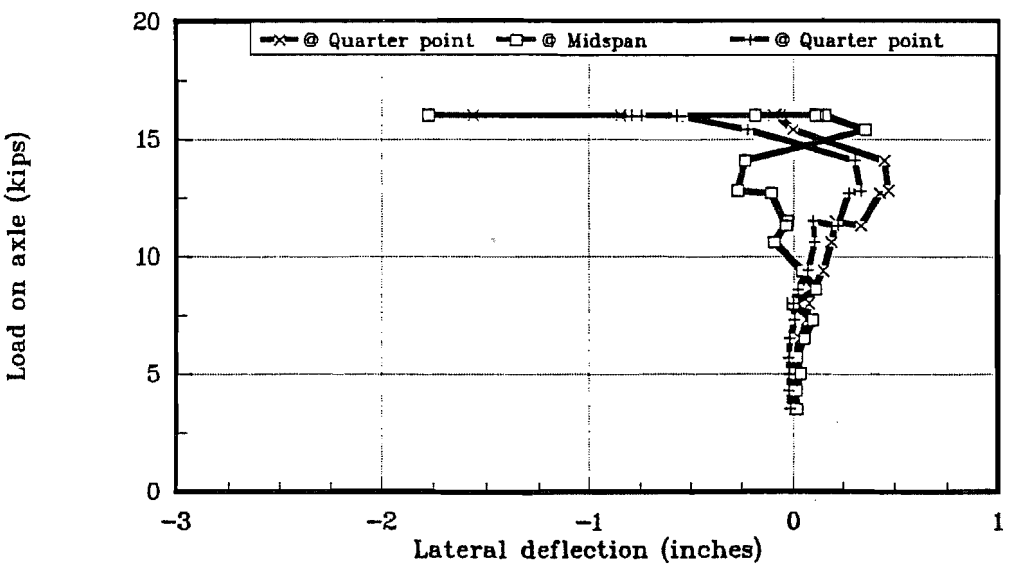

Figure 4.9 Lateral displacement curve for Beam #4.

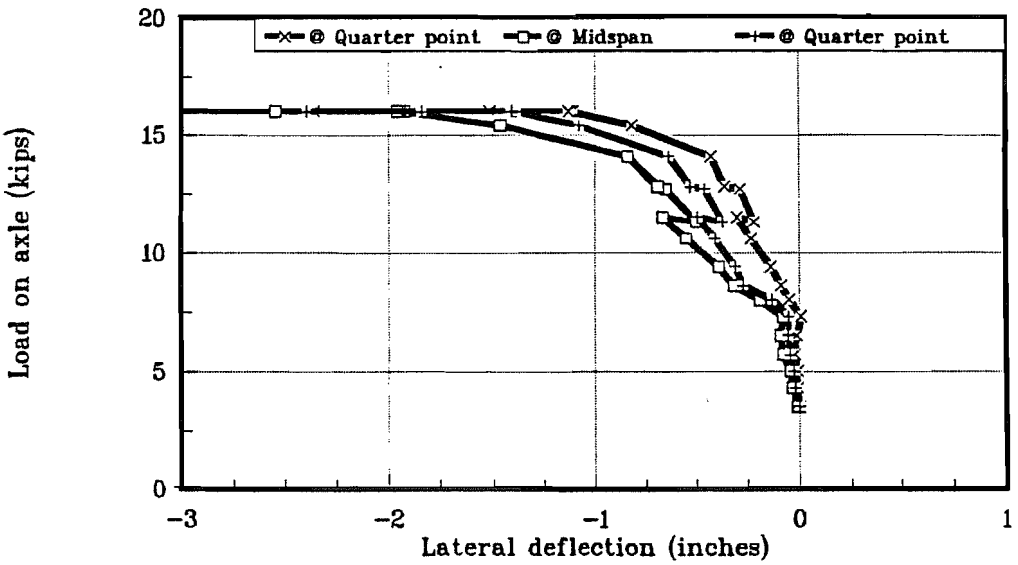

Figure 4.10 Lateral displacement curve for Beam #5.

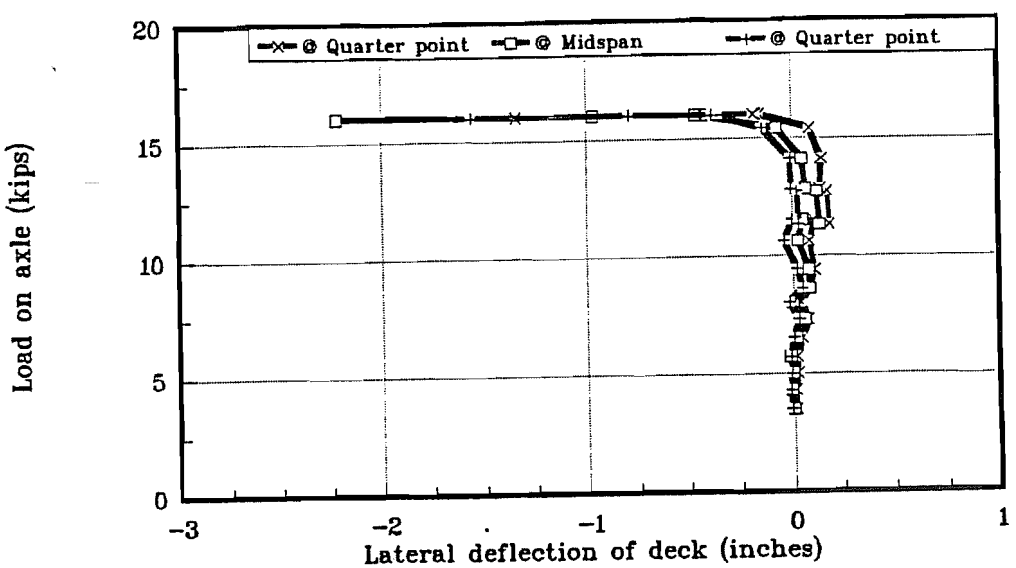

Figure 4.11 Lateral displacement curve of deck.

Figure 4.11 shows the lateral displacement curve for the deck. The positive x-direction implies movement of the deck toward the east, as shown in Figure 3.2. The deck did not show any lateral displacement until a load of 16.0 kips, after which it instantaneously moved laterally. When the bridge was unloaded, the deck exhibited elastic behavior and returned to its original straight position.

From the five lateral buckling curves of the beams, it can be seen that at loads lower than the buckling load, the beams show some midspan lateral displacements. This is consistent with the lateral displacement that would occur because of the deformed shape of the plank under the live load at midspan. Beams #1 and #2 are pushed toward the east, while Beams #4 and #5 are pushed toward the west. This also explains, to some extent, the fact that Beam #5 buckled earlier than Beam#1.

4.2.6 Observed Behavior During Test. The behavior observed at the different stages of loading are described in Table 4.1. During the test, it was observed that the beams started to buckle before the axle load reached midspan. As the axle load moved towards midspan, the moment was sufficient to cause buckling, since the unbraced length was greater than if the load were at midspan. This is clearly seen from Figure 4.12. The midspan lateral displacements, which were normalized to zero with the cart off the bridge, start increasing for the cart postion of 3 ft. As the load moved toward midspan, the displacements increased and the deck held the beams in the new deflected position.

From visual observation, the plank directly below the truck axle was not in full contact with the top flange of the beams as they buckled. The plank was bearing on the flange tip. Figure 4.13 shows Beam #3 in its buckled position with the plank resting on the

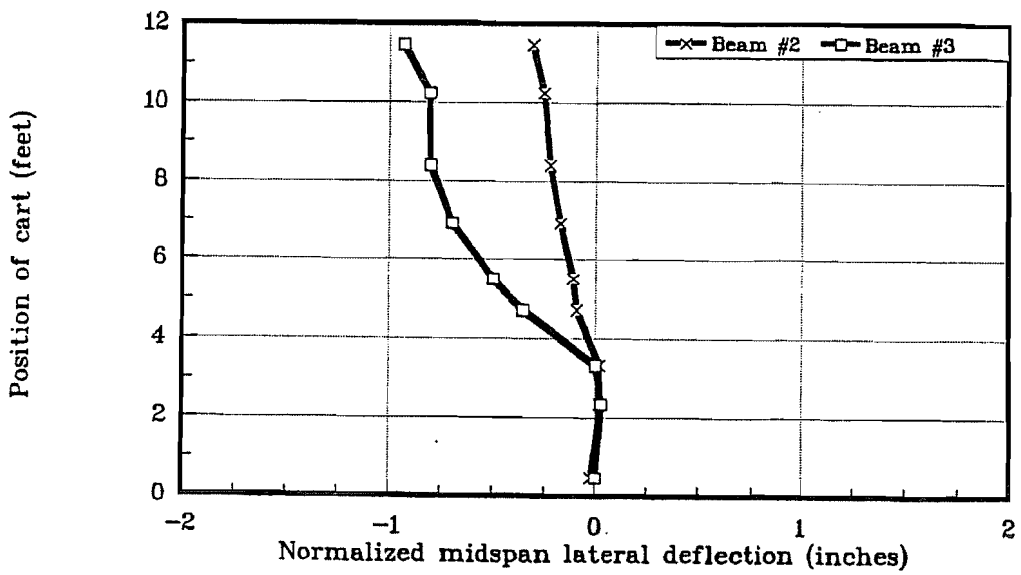

Figure 4.12 Graph showing position of cart at the start of buckling.

Table 4.1 Observed Behavior During Test

Load Level	Axle Load (kips)	Observed Behavior During Test
1	3.5	Vertical displacement of the beams increased linearly with load. No lateral movement was observed on the beams or the deck.
2	4.3	- Do -, Nailers started lifting off the deck
3	5.0	- Do -
4	5.7	- Do -
5	6.5	- Do -
6	7.3	Beam #3 shows some lateral movement
7	8.0	- Do -
8	8.6	- Do -
9	9.4	- Do -
10	10.6	- Do -
11	11.5	- Do -
12	12.8	Beam #3 buckled
13	14.1	- Do -
14	15.4	Beams #2, #4, and #5 start buckling. Yield lines were observed in the midspan region on the top right and bottom left flanges of beams #2, #3, #4 and #5.
15	16.0	Beam #1, #2, #3, #4, #5 experience lateral torsional buckling. Beams #2-5 touched safety supports below. Deck showed 2 in. lateral movement at midspan.
16	After the Test	Deck came back to initial straight position. The five beams showed a residual lateral displacement of 0, 1.44, 3.25, 1.25, 1.5 inches, respectively, at top flange midspan. Yield lines were observed in the midspan region of all the beam.

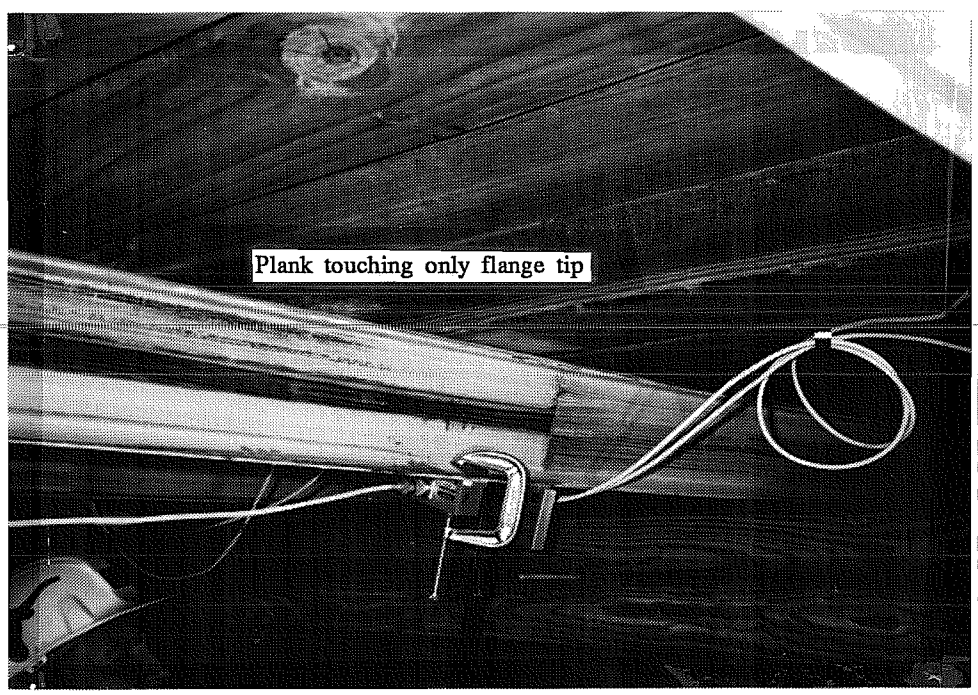

Figure 4.13 Photograph of Beam #3 in buckled position.

flange tip only. Figures 4.14a and 4.14b show the plank directly below the truck axle as the only one in contact with the beam.

Figure 4.16a is a photograph of the three interior beams in their buckled configuration after the test was done. The white string marks the original straight position of the beams. Figure 4.16b is a photograph showing the yield lines in the midspan region. The in-plane bending stresses superimposed on the out-of-plane stresses due to lateral torsional buckling cause the top and bottom flange tips on either side to yield.

4.3 Comparison and Discussion of Test Results

The following sections discuss the test results, with particular emphasis on load distribution and the expected capacity of the bridge.

4.3.1 Wheel Load Distribution. The transverse distribution of wheel loads among the stringers of a bridge is a function of the deck stiffness, beam stiffness, stringer spacing etc. The wheel load distribution controls the member size, and consequently, the strength and serviceability. Empirical wheel load distribution factors for stringers and longitudinal beams are given in the AASHTO Standard Specifications for Highway Bridges. But recent research findings (NCHRP Project 12-26) suggest a need to update these specifications to include more accurate predictions of wheel load distribution.

4.3.1.1 AASHTO Specifications. According to AASHTO, Standard Specifications for Highway Bridges, 1989, the distribution of wheel loads in longitudinal beams is specified in terms of a fraction of wheel load given in Table 3.23.1 of the AASHTO Manual. The distribution factors are a function of the deck material, the type of beams, and stringer spacing. For a timber deck, made of 4x8 planks, resting on steel stringers, the fraction of total wheel load a beam has to be designed for is S/4.5, where S is the stringer spacing.

For the test bridge, which has five stringers at a spacing of 3 feet, the distribution factor is 0.67, i.e., each stringer has to be designed for a load of 0.67 times the total wheel load or 0.33 times the axle load.

4.3.1.2 Structural Analysis. For the purpose of structural analysis, the bridge was idealized, as shown in Figure 4.17. The stiffness of the springs was taken as $48E_sI_s/L^3$ and the properties of the wood were measured by laboratory tests.

Using the principle of virtual work, the distribution of the wheel loads among the five beams was determined. Based on the reactions from the beams, the bending moment in the deck was determined. This ensured that the planks safely carried the load and did not

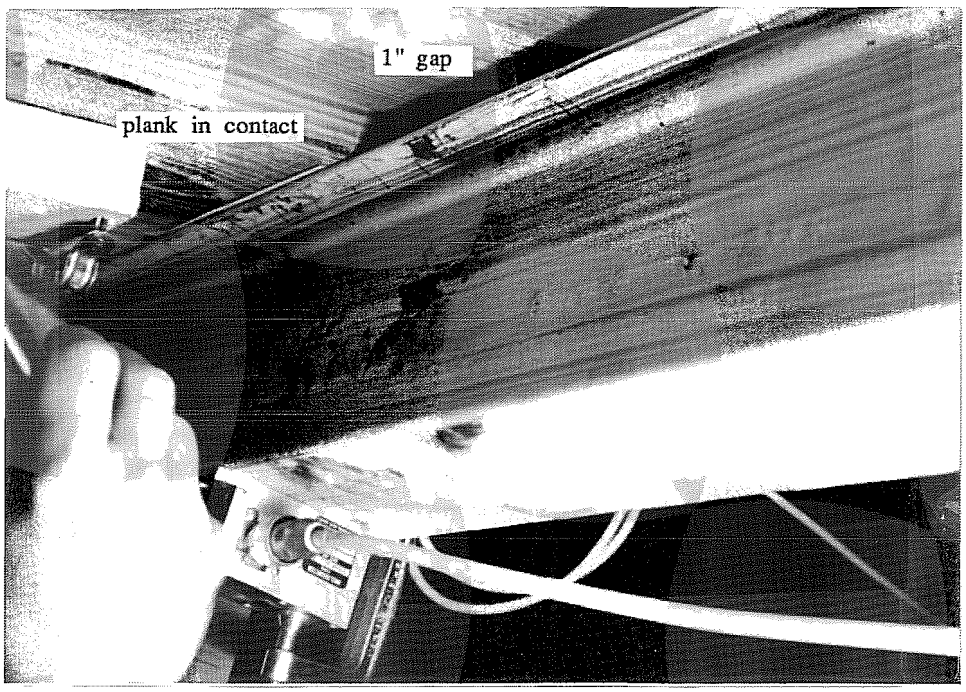

Figure 4.14a Photograph of plank in contact with beam.

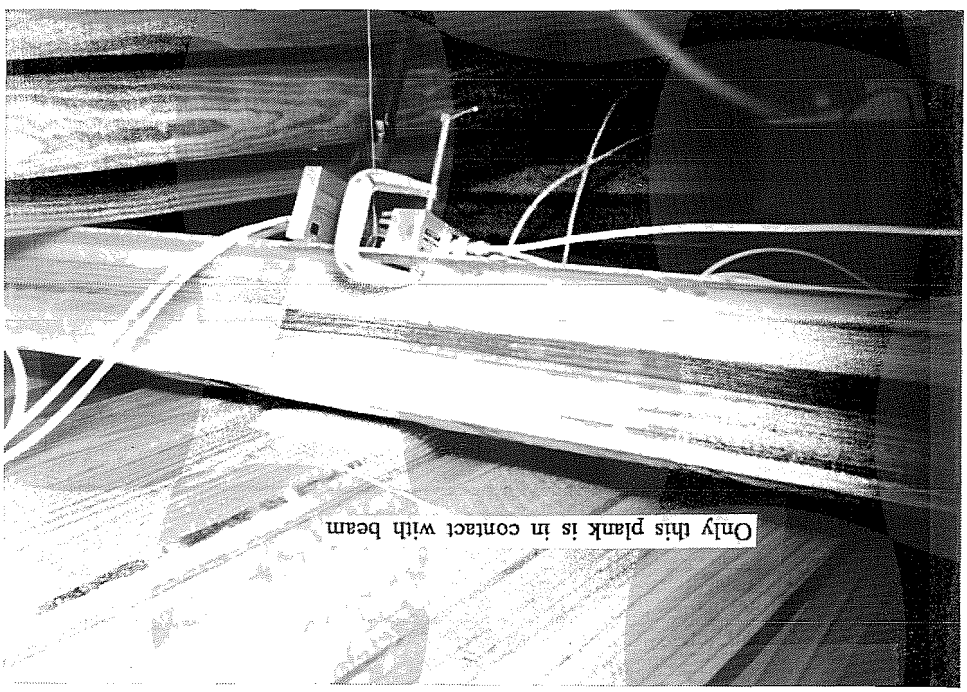

Figure 4.14b Photograph of plank below the truck axle.

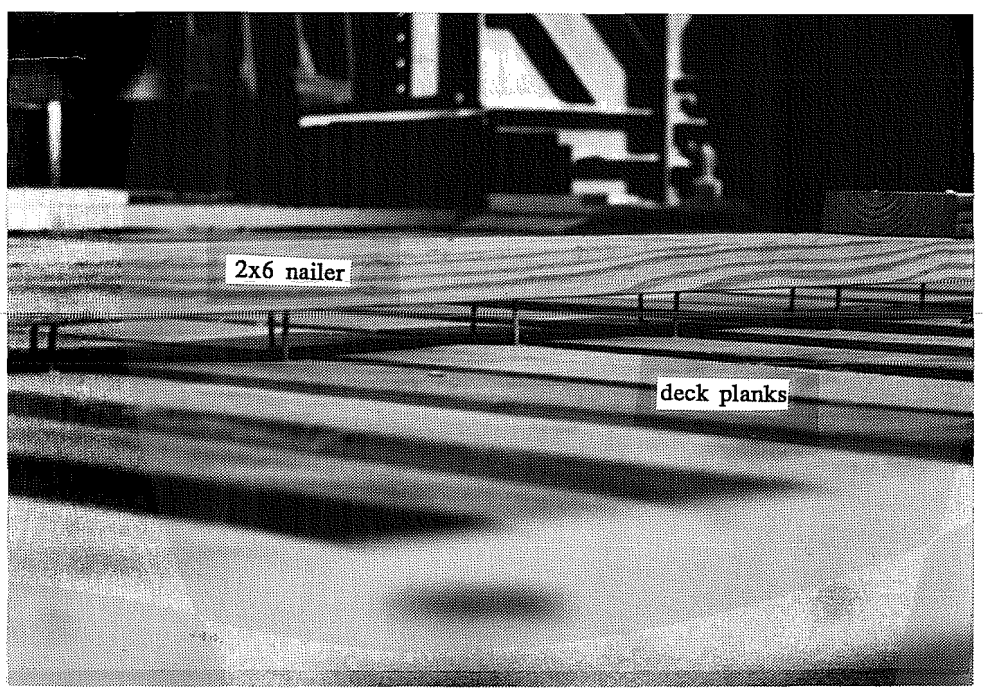

Figure 4.15 Photograph of nailer off the deck planks.

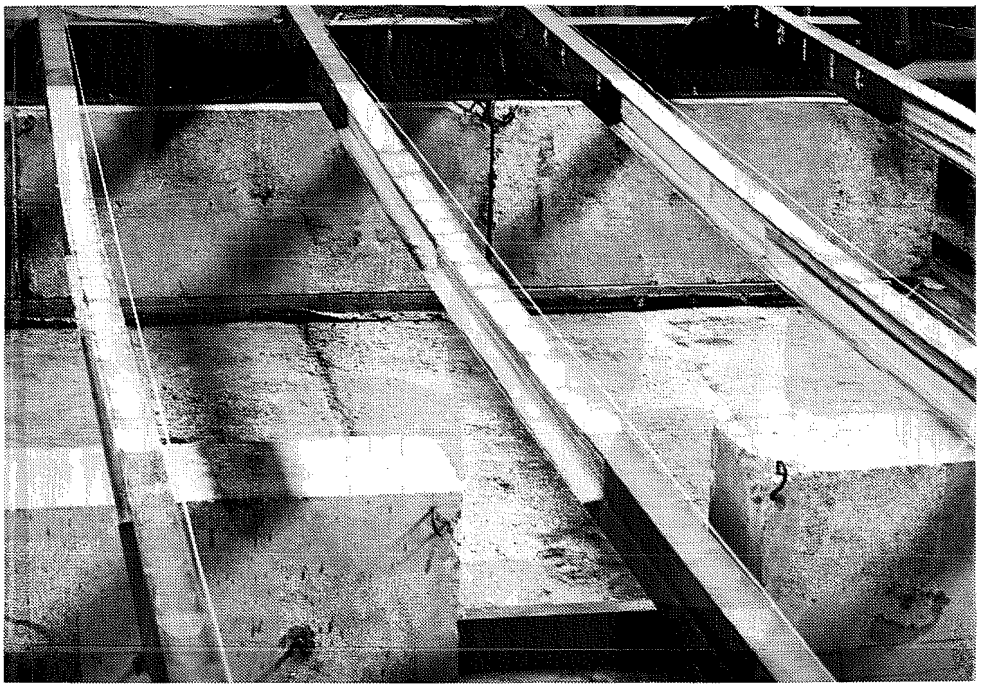

Figure 4.16a Deformed beams after the test.

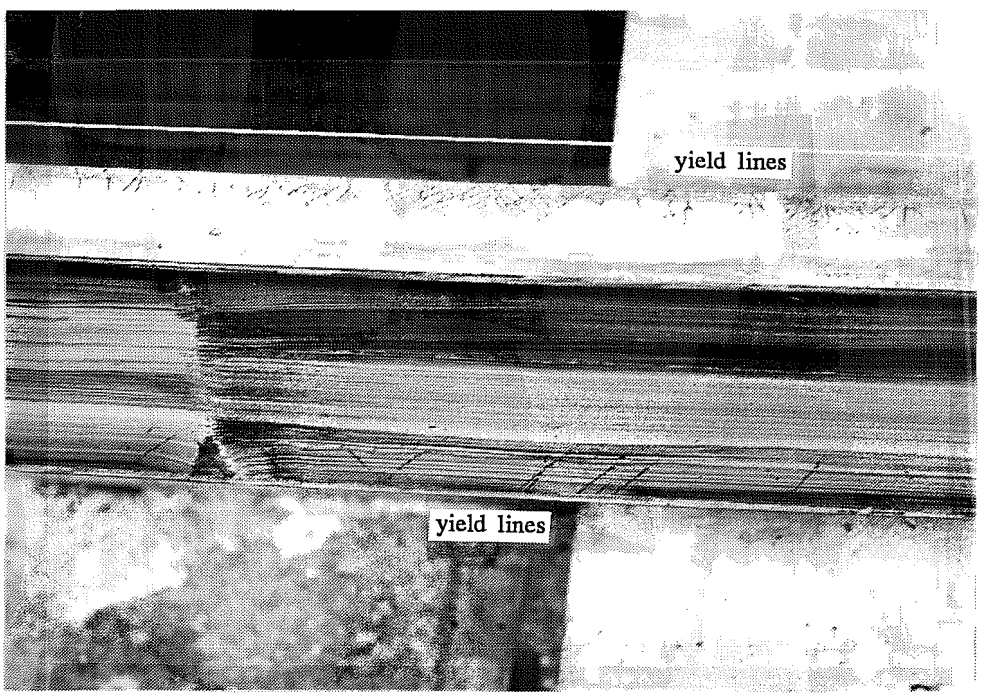

Figure 4.16b Photograph of yield lines on beam flange tips.

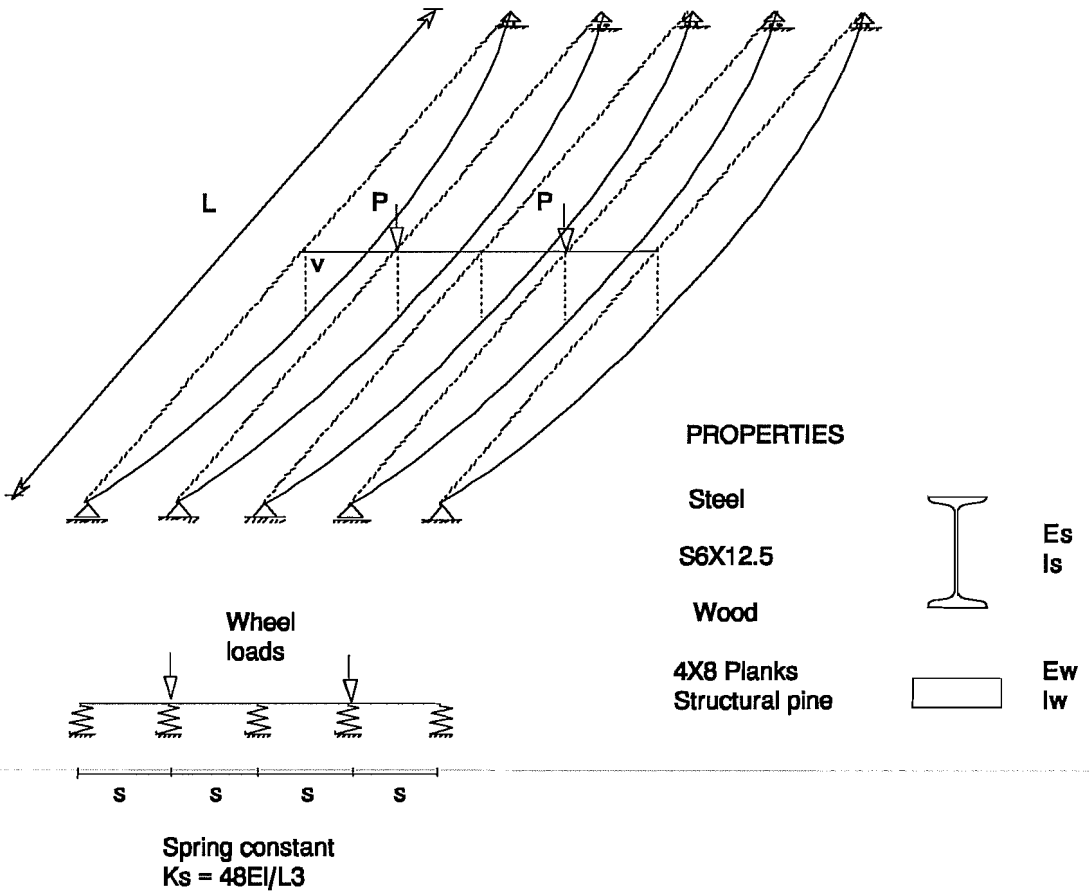

Figure 4.17 Idealization of the bridge.

control the failure of the bridge. The distribution of the loads is a function of the deck stiffness. A very flexible deck causes most of the wheel load to be carried by the beams right below it, while an infinitely stiff deck distributes the load equally among the five beams.

Table 4.2 Load Distribution Factors

Beam #	1	2	3	4	5
Load Factors	.125	.25	.25	.25	.125

The planks were assumed to be initially straight. Though this may not be true in the case of the bridge, the analysis gives an estimate of the stresses and forces in the bridge system. The distribution factors as a function of total load on the system determined from the above analysis are shown in Table 4.2. The analysis indicated that 75% of the axle load is supported equally by the three interior stringers.

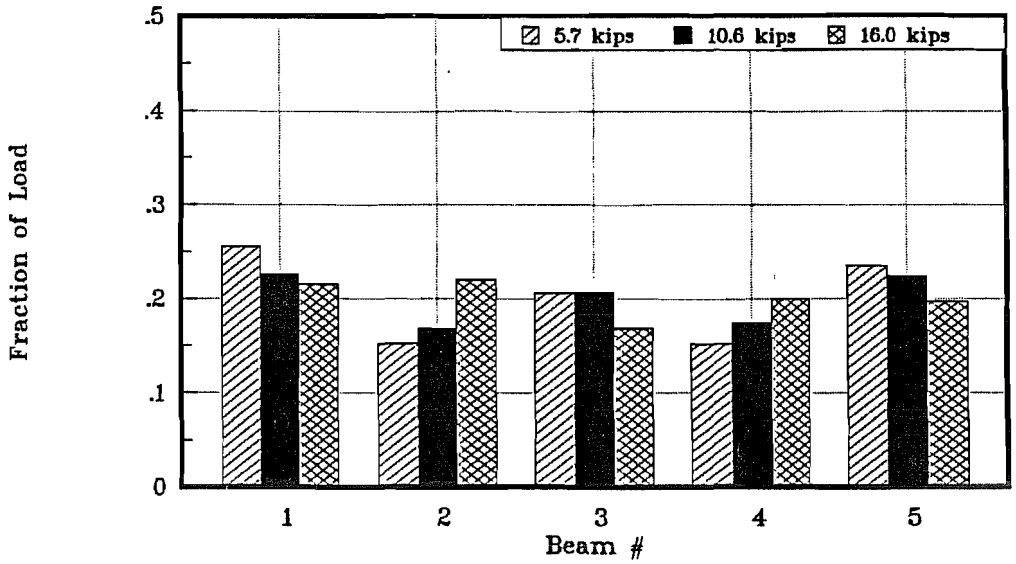

Figure 4.18 Total load distribution at different load levels.

4.3.1.3 Test Results. The total load distribution and live load distribution graphs for different load levels are shown in Figure 4.18 and Figure 4.19, respectively. On the y-axis is plotted the fraction of the total load carried by each beam. From the graphs it can be seen that the central three beams pick up most of the live load. Since the deck load is redistributed to the outer beams, the total load distribution shows a nearly uniform distribution among the five beams.

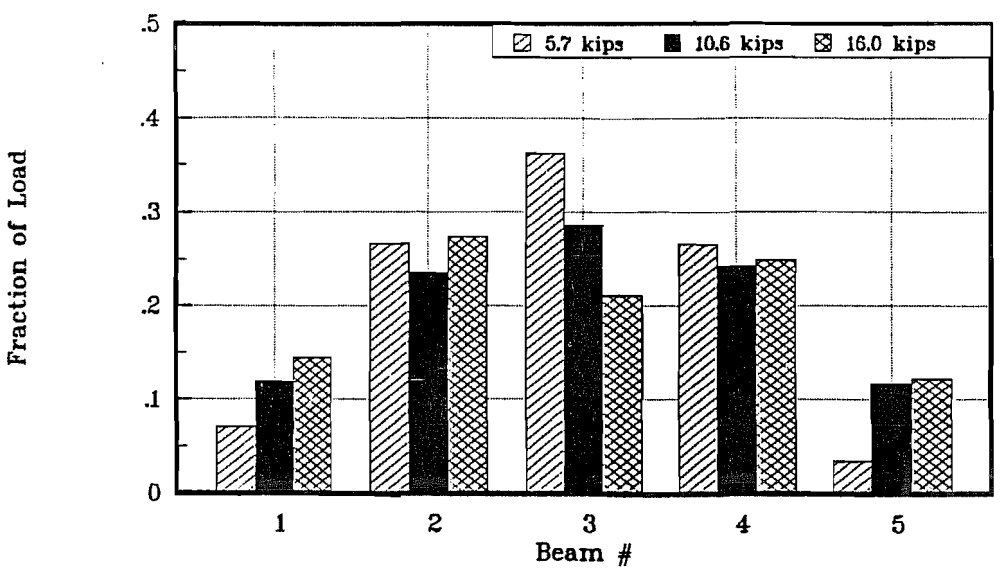

Figure 4.19 Live load distribution at different load levels.

The plots were done at different load levels to check if there is any change in load distribution as loads are increased. The total load distribution and the live load distribution remained nearly constant at lower load levels. At the ultimate load of 16 kips, Beam #3 shedded load to the other beams as it lost in-plane stiffness due to its earlier lateral buckling compared to the other beams.

Figure 4.20 shows a comparison of the total load distribution factors as determined from the experiment (at 10.6 kips), AASHTO specifications and structural analysis. As compared to the experiment, the AASHTO specifications are conservative. The structural analysis gives closer results for the three interior beams. The difference on the exterior beams is due to redistribution of the deck load when the cart comes on to the bridge. This is not considered in the analysis. In the case of the test bridge, the deck load is a significant portion (13%) of the total capacity of the bridge. The deck size is significant compared to the size of the beams. The almost uniform distribution from the test may be partly due to the comparable deck and beam in-plane stiffness.

4.3.2 Capacity of the Test Bridge. The capacity of the bridge as measured from the experiment was 16.0 kips (axle load)+ weight of the deck. The deck weighed 4 kips. Since it is a uniformly distributed load, it is equivalent to 0.5 × 4 kips as a concentrated load. Therefore, the ultimate capacity is 18.0 kips.

The following section shows the calculations of the Inventory Rating of the Test bridge as determined by the Texas Bridge Load Rating Program. The allowable stress formulas have been used.

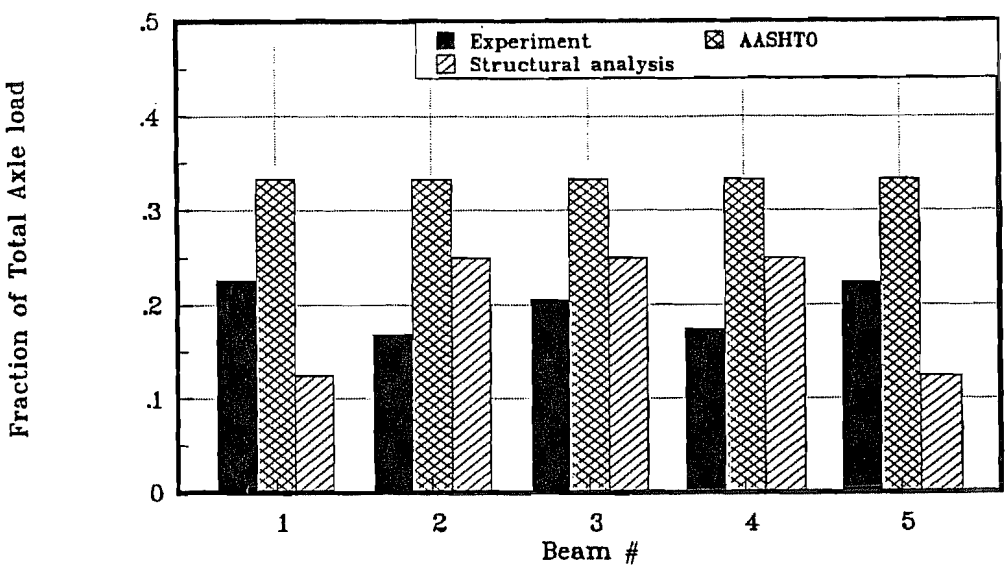

Figure 4.20 Comparison of load distribution factors.

4.3.2.1 Texas Bridge Load Rating Program

1)	Span type	24.0 ft.
3)	Stringer spacing	3.0 ft.
4)	Stringer designation	S6 x 12.5
5)	Stringer section modulus	7.4 in^3
6)	Stringer weight	0.013 k/ft
7)	Corrosion loss	0%
8)	Yield strength	42.1 ksi
9)	Unbraced length	24 ft.
10)	Flange width	3.33 in.
11)	Deck type	Treated timber plank
12)	Deck thickness	4.0 in.
13)	Timber unit weight	0.050 k/ft^3
14)	Surfacing	Timber runners
15)	Surfacing thickness	0.125 in.
16)	Number of lanes on bridge	1
17)	Live load impact factor	1.3 (As per AASHTO 1989, Standard Specifications for Highway Bridges, Article 3.8.2.1)

Using the procedure adopted by the program:

1) Using the conservative lateral buckling formula of AASHTO, 1983,

Allowable bending stress (see Eq. 3), $F_b = A - B\left(L_b / b\right)^2$

$$F_b = .55\left(42.1\right) - 0.0102\left(24 \times 12 / 3.33\right)^2$$

$$= -53.1 \text{ ksi. (negative value)}$$

M_{ALL} = Allowable stress x section modulus

$$= -53.1 \times 7.37$$

$$= -391.6 \text{ k-in} = -32.6 \text{ k-ft}$$

Calculation of dead load moment:

a) Deck weight = $4 \times 3 / \left(24 \times 16\right) = 0.03$ k/ft.

(Measured weight of deck= 4 kips; size of deck is 16 ft. x 24 ft.; stringer spacing = 3 ft)

b) Stringer = 0.013 k/ft

Total dead weight = 0.043 k/ft

$$M_{DL} = \frac{wL^2}{8} = \frac{0.0043 \times 24.0^2}{8} = 3.1 \text{ k-ft}$$

M_{LL} = Impact factor x load distribution factor x H15 wheel load moment

$$= \quad 1.3 \times \frac{3}{4.5} \times \left[\frac{12 \times 24}{4} \right]$$

$$= \quad 62.4 \text{ k-ft}$$

$$\text{Inventory Rating} \quad = \quad H15 \left[\frac{M_{ALL} - M_{DL}}{M_{LL}} \right]$$

$$= \quad H15 \left[\frac{-32.6 - 3.1}{62.4} \right]$$

$$= \quad - H8.6$$

As can be seen, the 1983 formula gives a unrealistic estimate of the bridge capacity. If the midspan was assumed braced, the capacity would be H0.24.

2) Using the AASHTO 1990 lateral buckling formula,

$$M_{ALL} = 50 \times 10^3 C_b \frac{I_{yc}}{L_b} \sqrt{0.772 \frac{J}{I_{yc}} + 9.87 \left(\frac{d}{L_b} \right)^2} < 0.55 M_y$$

$$M_{ALL} = 50 \times 10^3 \times 1.0 \times \frac{0.91}{288} \sqrt{0.772 \frac{0.17}{0.91} + 9.87 \left(\frac{6}{288} \right)^2} < 14.2 \text{ k-ft}$$

M_{ALL} = 60.9 k-in = 5.07 k-ft

M_{DL} = 3.1 k-ft

M_{LL} = 62.4 k-ft

$$\text{Inventory Rating} \quad = \quad H15 \left[\frac{M_{ALL} - M_{DL}}{M_{LL}} \right]$$

$$= \quad H15 \left[\frac{5.07 - 3.1}{62.4} \right]$$

$$= \quad H0.47$$

The new formula gives a better estimate of the bridge capacity but is still conservative because no bracing is assumed along the span. If the midspan is assumed braced, the capacity would be H3.7 with C_b = 1.75. But yielding controls, so the capacity would be limited by the yield capacity which is H2.7.

3) The actual ultimate live load capacity of the bridge was 16.0 kips. In terms of the Inventory Rating, the test load would be equivalent to

$$= \text{H15} \times \frac{\text{Ultimate live load}}{\text{H15 axle load}} \times \frac{1}{\text{Factor of safety}}$$

$$= \text{H15} \times \frac{16.0}{24.0} \times \frac{1}{1.8} \times \frac{1}{1.3} \times \frac{0.2}{0.33}$$

(Impact factor = 1.3, 0.2/0.33 accounts for difference in load distribution factors).

$$= \text{H2.56}$$

Therefore, if the bridge were assumed as braced at midspan, the rating would be slightly unconservative. The results are summarized in Table 4.3.

Table 4.3 Comparison of Inventory Ratings

Inventory Rating	AASHTO 1983	AASHTO 1990	Bridge Test
No Brace	-H8.6	H0.47	H2.56
Brace at midspan	H0.24	H2.7	—

4.3.2.2 Comparison of Test Bridge Capacity with BASP Results. In this section, the BASP results used to quantify the bracing effect of the deck on the capacity of the bridge are presented. Figure 4.21 shows the single beam capacities for different modes of failure as predicted by BASP, design equations, and the experiment.

BASP was used to calculate the braced capacity of the bridge beams. This involved specifying a brace type and brace stiffness. From the test, it is clear that the bridge beams were braced. Different types of braces and brace stiffness were used in an attempt to

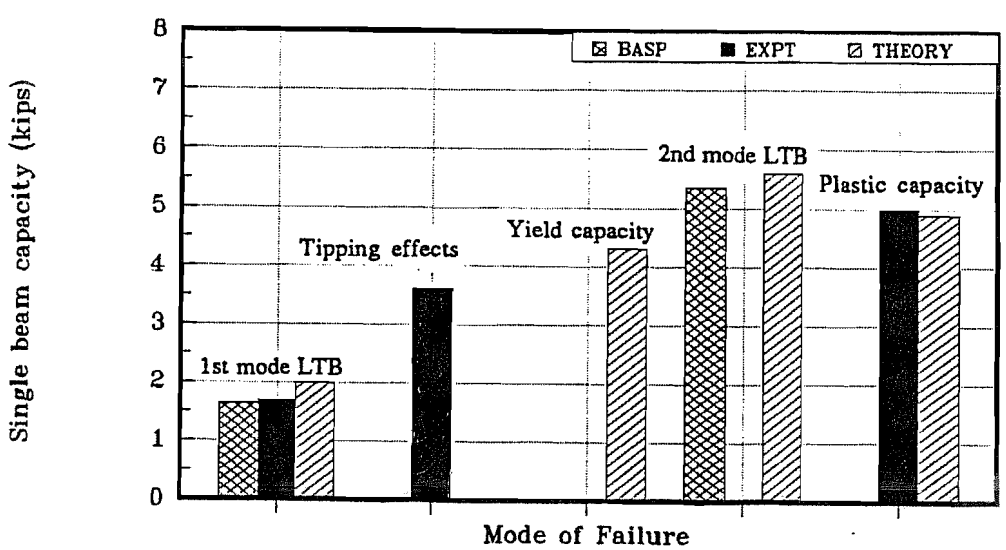

Figure 4.21 Single beam capacities.

quantify the bracing effect. From lateral deck stiffness tests (Webb, 1991), the lateral stiffness was experimentally determined. This gave a lateral stiffness of 0.25 k/in per beam. If this was assumed as a lateral brace at midspan, the single beam capacity was 3.3 kips as opposed to the single beam capacity of 3.7 kips from the bridge test. Assuming that the deck provided torsional restraint of 6EI/L at midspan gave full bracing and the yield capacity of 4.3 kips controlled. These results are presented in graphical form in Figure 4.22. The bridge capacity was taken as 5 times the single beam capacity.

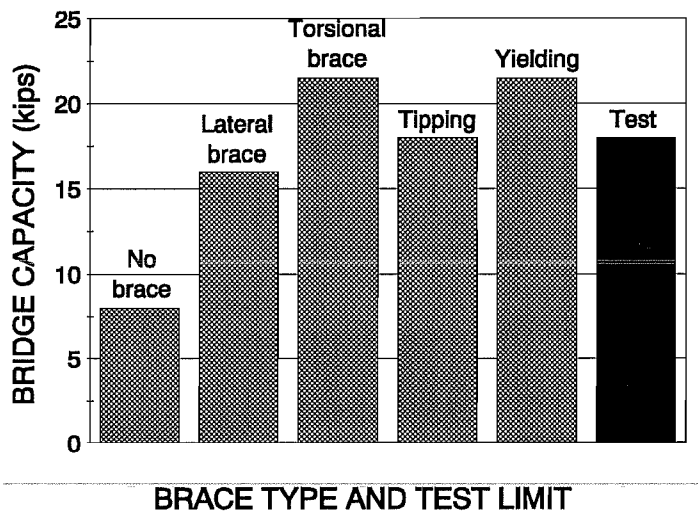

Figure 4.22 BASP results for bridge capacities.

Figure 4.22 shows that it is conservative to rely on the lateral bracing stiffness of the deck to brace the beam at the load pooint. Some relative movement between the deck and the stringers did occur but it is not clear that this movement can be classified as slip. Figure 4.12 shows that midspan lateral movement of the interior stringers occurred before the midspan plank made contact with the steel stringers. It is unconservative to assume that the deck can provide a torsional stiffness of 6EI/S because the planks were only bearing on the flange tips. The maximum bridge load, however, compares closely to the tipping effect load determined by the twin beam experiments. As observed from the preliminary tests, tipping effects raised the beam capacity by a factor of 2. The same increase was noted from the bridge test, as seen from Figure 4.22. Considering only the tipping effect, the bridge capacity would be 5x3.6 = 18.0 kips, which is the same as the 18.4 kips maximum bridge load. The relative contribution of lateral bracing and tipping effects cannot be established from the experiment.

Chapter 5
CONCLUSIONS AND RECOMMENDATIONS

5.1 Summary

A full scale laboratory test was conducted on a 24-ft-span multi-girder bridge comprised of five steel stringers supporting a timber plank deck. The bridge was loaded until failure with a moving load system composed of a standard truck axle and a cart loaded with concrete blocks. The bridge system was instrumented with strain gauges, vertical displacement gauges, and lateral displacement gauges. The objective was to study the lateral instability of the steel stringers and to evaluate the bracing effect of the bridge deck.

Preliminary tests were conducted on individual beams to study single beam behavior. The computer program BASP and the design equations were used to arrive at theoretical values.

5.2 Conclusions

The ultimate load carried by the bridge indicated that the beams were partially braced by the deck. The bracing was mainly due to some lateral restraint provided by the friction mobilized at the deck beam interface and torsional restraint due to tipping effects. It was observed from the test that the deck was in full contact with the beam only at the location of the wheel load. Hence, there can be restraint only at the wheel location. As the beams tried to buckle there was loss in contact between the top flange of the beams and deck except at the flange tips. Hence, the torsional restraint of 6EI/L cannot be assumed though there is help from tipping effects. At the midspan, the interior beams move relative to the decks but this lateral movement occurred before the load reached midspan.

The design equations can be used to arrive at the improved capacity of the beams due to the effects of bracing. This requires the quantification of the bracing effect in terms of a brace stiffness, which is beyond the scope of this report.

5.3 Design Guidelines

1) The Bridge Rating Manual needs to be updated to use the new AASHTO 1990 lateral buckling formula.

2) The load distribution factors given by the AASHTO bridge specifications are conservative, more realistic factors would result in better utilization of bridges. For example, when assessing lateral buckling, all five girders must buckle before collapse.

Consequently, the load rating could be calculated using the five girders, rather than the 3.3 girders specified in the AASHTO load distribution factors.

3) The bracing provided by the bridge deck is a significant contribution to the overall capacity of the bridge. The bridge test showed that the capacity was twice the unbraced capacity. In order to evaluate the bracing effect, the lateral restraint provided by the deck must be assessed.

5.4 Suggested Implementations

The results of the experimental work gave valuable insight into the subject of beam bracing. The full scale test demonstrated the ability of the bridge deck to brace the beams so that they could reach a higher buckling stress than predicted by conventional analysis. This helps bridge engineers rating short span bridges to confidently estimate the strength of the stringers, thus eliminating low ratings because of lateral instability.

This would increase the allowable wheel loads on bridges, thus improving the usefulness of the bridge and avoiding unnecessary posting or rehabilitation. The results can be incorporated in bridge rating manuals and the AASHTO bridge specifications. The information would also eliminate costly and unnecessary attachment details on new structures.

APPENDIX A
Laboratory Test Data

Load Level	Axle Load	Position of Cart	load per beam #1	load per beam #2	load per beam #3	load per beam #4	load per beam #5
	(kips) WS#1+#2	(inches) PG	(kips) CAL	(kips) CAL	(kips) CAL	(kips) CAL	(kips) CAL
1	3.5	-11.4	.206	.277	.154	.003	.015
	3.5	88.1	.601	.569	.518	.536	.652
	3.5	144.5	.643	.633	.605	.640	.576
2	4.3	-11.3	.124	.314	.181	.143	.073
	4.3	59.5	.804	.700	.688	.666	.963
	4.3	143.6	.776	.807	.713	.783	.691
3	5.0	-11.9	.210	.444	.078	.147	.104
	5.0	74.4	.923	.819	.752	.770	.984
	5.0	144.6	.945	.921	.877	.935	.836
4	5.7	-9.4	-.047	.559	.122	.173	.158
	5.7	61.3	1.114	.984	.944	.955	1.239
	5.7	144.6	1.064	1.083	1.000	1.088	.953
5	6.5	-12.1	.183	.610	-.063	.028	.017
	6.5	91.1	1.215	1.253	1.036	1.145	1.286
	6.5	143.5	1.166	1.226	1.162	1.287	1.156
6	7.3	-11.0	.013	.638	.076	-.074	.016
	7.3	72.7	1.479	1.343	1.222	1.348	1.589
	7.3	143.3	1.439	1.437	1.305	1.362	1.199
7	8.0	-8.7	.143	.881	-.261	-.208	-.079
	8.0	86.0	1.593	1.641	1.585	1.737	1.831
	8.0	144.0	1.484	1.524	1.451	1.579	1.385
8	8.6	-12.3	-.018	.799	-.219	-.290	-.247
	8.6	88.8	1.665	1.736	1.535	1.698	1.796
	8.6	144.4	1.571	1.648	1.554	1.665	1.469
9	9.4	-12.9	.338	.972	-.104	-.091	-.061
	9.4	96.1	1.731	1.776	1.687	1.780	1.905
	9.4	143.6	1.750	1.876	1.697	1.759	1.599
10	10.6	-10.0	.284	1.268	-.621	-.476	-1.633
	10.6	76.1	2.075	1.878	1.837	2.059	2.251
	10.6	143.9	1.896	2.053	1.999	2.147	1.952
11	11.5	3.4	5.999	-2.041	4.845	3.368	3.911
	11.5	77.5	2.294	2.129	2.152	2.394	2.480
	11.5	143.6	2.061	2.257	2.201	2.344	2.108
12	12.7	1.5	17.732	15.673	13.332	7.089	7.644
	12.7	73.8	2.580	2.742	2.399	2.691	2.833
	12.7	141.5	2.344	2.781	2.505	2.639	2.322
13	12.8	3.5	8.260	9.390	6.166	3.763	5.468
	12.8	96.2	2.250	2.860	2.504	2.670	2.537
	12.8	141.5	2.263	2.750	2.479	2.708	2.421
14	14.1	7.2	5.581	6.277	4.132	2.942	4.029
	14.1	72.7	2.869	3.235	2.476	2.867	2.808
	14.1	136.4	2.500	3.176	2.779	2.825	2.494
15	15.4	5.5	6.250	9.547	3.910	4.345	5.095
	15.4	82.9	3.309	3.837	2.533	3.014	2.685
	15.4	137.5	2.942	3.800	2.644	3.244	2.565
16	16.0	21.7	3.985	5.198	2.261	3.461	3.836
	16.0	40.7	3.388	4.069	2.007	3.140	3.423
	16.0	67.1	3.078	3.857	2.271	3.138	2.961
	16.0	83.4	3.085	4.100	2.628	3.357	2.986
	16.0	103.5	2.954	3.992	2.545	3.623	2.942
	16.0	124.8	2.987	4.287	2.677	3.629	2.756
	16.0	137.9	2.977	4.016	2.435	3.627	2.691
	16.0	99.8	2.925	3.972	2.124	3.236	2.584
	16.0	79.6	3.373	3.937	2.070	3.118	2.783
	16.0	40.7	3.734	4.184	1.920	3.272	3.159
	16.0	45.1	3.395	4.172	1.830	3.337	3.511
	16.0	73.1	3.198	4.125	2.412	3.698	3.218
	16.0	112.6	3.158	4.336	2.164	3.791	2.832
	16.0	137.0	3.711	4.084	1.348	3.313	2.170
	16.0	138.3	3.661	3.958	1.251	3.169	2.065
	16.0	97.1	3.616	3.926	1.157	3.011	2.384

Load Level	Axle Load	Position of Cart	Vertical deflection @ Midspan				
			#1	#2	#3	#4	#5
	(kips) WS#1+#2	(inches) PG	(inches) VG 1	(inches) VG 2	(inches) VG 3	(inches) VG 4	(inches) VG 5
1	3.5	-11.444	.013	.049	.006	.016	.020
	3.5	88.093	-.320	-.330	-.384	-.381	-.319
	3.5	144.468	-.442	-.442	-.505	-.526	-.388
2	4.3	-11.270	.002	.048	.000	.010	.020
	4.3	59.501	-.263	-.235	-.309	-.288	-.256
	4.3	143.602	-.551	-.576	-.622	-.654	-.462
3	5.0	-11.932	.015	.044	.009	.012	.024
	5.0	74.421	-.396	-.451	-.486	-.470	-.392
	5.0	144.588	-.631	-.678	-.740	-.771	-.575
4	5.7	-9.352	-.026	-.211	-.028	-.011	.008
	5.7	61.287	-.366	-.604	-.440	-.411	-.358
	5.7	144.565	-.741	-1.015	-.867	-.906	-.669
5	6.5	-12.076	.020	-.245	-.001	.005	.015
	6.5	91.133	-.629	-1.025	-.779	-.789	-.630
	6.5	143.454	-.831	-1.184	-.993	-1.030	-.775
6	7.3	-10.960	.013	-.490	-.003	.009	.014
	7.3	72.748	-.573	-1.041	-.694	-.692	-.550
	7.3	143.333	-.955	-1.381	-1.112	-1.142	-.854
7	8.0	-8.735	.003	-.155	-.014	-.003	.001
	8.0	86.041	-.721	-.932	-.857	-.890	-.687
	8.0	143.975	-1.007	-1.274	-1.221	-1.293	-.975
8	8.6	-12.300	.023	-.307	-.017	-.012	-.009
	8.6	88.810	-.842	-1.242	-1.014	-1.031	-.805
	8.6	144.372	-1.093	-1.560	-1.319	-1.375	-1.074
9	9.4	-12.949	.033	-.441	-.001	.002	-.002
	9.4	96.097	-.902	-1.685	-1.188	-1.210	-.949
	9.4	143.599	-1.233	-1.791	-1.423	-1.431	-1.127
10	10.6	-9.961	.023	.007	-.008	-.006	-.009
	10.6	76.138	-.887	-1.112	-1.198	-1.245	-.949
	10.6	143.889	-1.326	-1.608	-1.668	-1.750	-1.407
11	11.5	3.445	-.114	-.386	-.142	-.120	-.095
	11.5	77.541	-.932	-1.387	-1.228	-1.289	-.990
	11.5	143.582	-1.430	-1.896	-1.833	-1.924	-1.539
12	12.7	1.452	-.914	-1.286	-1.124	-1.097	-.836
	12.7	73.832	-.444	-.693	-.517	-.528	-.362
	12.7	141.548	-1.378	-2.128	-2.002	-1.994	-1.513
13	12.8	3.548	-1.459	-2.218	-2.149	-2.128	-1.657
	12.8	96.155	-.458	-.940	-.565	-.624	-.411
	12.8	141.543	-1.350	-2.398	-2.058	-2.088	-1.587
14	14.1	7.201	-1.439	-2.473	-2.185	-2.148	-1.666
	14.1	72.669	-.306	-.810	-.401	-.341	-.263
	14.1	136.428	-1.593	-2.692	-2.342	-2.275	-1.648
15	15.4	5.472	-1.648	-2.741	-2.411	-2.372	-1.742
	15.4	82.900	-1.239	-1.897	-1.595	-1.519	-1.070
	15.4	137.474	-1.778	-2.789	-2.576	-2.350	-1.571
16	16.0	21.705	-.043	-.437	-.131	-.065	-.057
	16.0	40.651	-.260	-.736	-.384	-.296	-.242
	16.0	67.134	-.969	-1.783	-1.479	-1.409	-1.125
	16.0	83.407	-1.304	-2.279	-2.040	-1.923	-1.388
	16.0	103.481	-1.303	-2.285	-2.040	-1.926	-1.389
	16.0	124.797	-1.533	-2.497	-2.336	-2.193	-1.540
	16.0	137.933	-1.912	-3.286	-2.967	-2.812	-2.077
	16.0	99.756	-2.120	-3.353	-3.225	-3.032	-2.353
	16.0	79.557	-2.117	-3.402	-3.276	-3.074	-2.416
	16.0	40.690	-1.629	-2.815	-2.755	-2.477	-1.834
	16.0	45.105	-.702	-1.273	-.920	-.926	-.695
	16.0	73.141	-.300	-.809	-.395	-.374	-.324
	16.0	112.637	-.911	-1.635	-1.416	-1.343	-1.078
	16.0	137.041	-1.289	-2.224	-2.004	-1.855	-1.366
	16.0	138.255	-1.942	-3.124	-2.986	-2.738	-2.000
	16.0	97.092	-2.401	-3.661	-3.368	-3.333	-2.600

Load Level	Axle Load	Position of Cart	Lateral deflection of Wood Deck		
			Quarter pt	Midspan	Quarter pt
	(kips) WS#1+#2	(inches) PG	(inches) LG A	(inches) LG B	(inches) LG C
1	3.5	-11.444	-.001	-.003	.000
	3.5	88.093	-.002	.008	.014
	3.5	144.468	-.010	.000	.009
2	4.3	-11.270	.000	-.004	-.001
	4.3	59.501	-.003	.000	.007
	4.3	143.602	-.009	.010	.013
3	5.0	-11.932	-.003	-.007	-.003
	5.0	74.421	-.005	.007	.015
	5.0	144.588	-.019	.005	.010
4	5.7	-9.352	-.004	-.006	.001
	5.7	61.287	-.008	-.001	.012
	5.7	144.565	-.014	.017	.016
5	6.5	-12.076	-.014	-.027	-.015
	6.5	91.133	-.031	-.013	-.003
	6.5	143.454	-.041	-.013	-.001
6	7.3	-10.960	-.011	-.023	-.010
	7.3	72.748	-.033	-.024	-.005
	7.3	143.333	-.072	-.055	-.026
7	8.0	-8.735	-.007	-.017	-.001
	8.0	86.041	-.037	-.018	-.006
	8.0	143.975	-.038	.003	.018
8	8.6	-12.300	-.036	-.084	-.051
	8.6	88.810	-.079	-.094	-.065
	8.6	144.372	-.076	-.079	-.044
9	9.4	-12.949	-.038	-.065	-.010
	9.4	96.097	-.061	-.031	.009
	9.4	143.599	-.106	-.076	-.020
10	10.6	-9.961	-.030	-.036	.038
	10.6	76.138	-.071	-.035	.026
	10.6	143.889	-.080	-.024	.040
11	11.5	3.445	-.058	-.075	-.024
	11.5	77.541	-.084	-.050	-.007
	11.5	143.582	-.103	-.046	.001
12	12.7	1.452	-.060	-.083	-.015
	12.7	73.832	-.086	-.028	.013
	12.7	141.548	-.168	-.118	-.024
13	12.8	3.548	-.057	-.060	.011
	12.8	96.155	-.092	-.024	.024
	12.8	141.543	-.134	-.064	.005
14	14.1	7.201	-.071	-.082	-.012
	14.1	72.669	-.096	-.037	-.003
	14.1	136.428	-.141	-.048	.006
15	15.4	5.472	-.100	-.140	-.059
	15.4	82.900	-.298	-.302	-.095
	15.4	137.474	-.087	.073	.143
16	16.0	21.705	-.129	-.184	-.066
	16.0	40.651	-.119	-.141	-.033
	16.0	67.134	-.125	-.100	-.014
	16.0	83.407	-.151	-.100	-.019
	16.0	103.481	-.048	.103	.201
	16.0	124.797	.062	.312	.347
	16.0	137.933	.155	.430	.356
	16.0	99.756	.211	.487	.507
	16.0	79.557	.133	.310	.401
	16.0	40.690	.067	.082	.202
	16.0	45.105	-.031	-.014	.084
	16.0	73.141	-.066	-.008	.099
	16.0	112.637	.022	.258	.394
	16.0	137.041	.432	.969	.794
	16.0	138.255	1.341	2.223	1.561
	16.0	97.092	1.254	1.999	1.753

Note:

1) CAL refers to values calculated from the gauge data.

2) The positive values of deck lateral deflection refer to movement towards east.

BIBLIOGRAPHY

1. Akay, H.U., Johnson, C.P., and Will, K.M., "Lateral and Local Buckling of Beams and Frames," Journal of the Structural Division, ASCE, September 1977.

2. American Association of State Highway and Transportation Officials (AASHTO), Standard Specifications for Highway Bridges, 1983.

3. American Association of State Highway and Transportation Officials (AASHTO), Standard Specifications for Highway Bridges, Interim Report 1990.

4. Flint, A.R., "The Stability of Beams loaded through Secondary members", Civil Engineering and Public Works Review, Vol 46

5. Kirby, P.A. and Nethercot, D.A., Design for Structural Stability, 1979.

6. Kissane, R.J., "Lateral Restraint of Non-composite Beams", Research report 123, New York State Department of Transportation.

7. Texas Bridge Load Rating Program, User's Manual, State Department of Highways and Public Transportation, Bridge Division, December 1988.

8. Timoshenko, S., and Gere, J.,Theory of Elastic Stability, McGraw Hill Book Company, 1961.

9. Webb, S. and Yura, J.A., "Evaluation of Stiffness of Bridge Decks" Report No. 1239-3, Center for Transportation Research, The University of Texas at Austin, September, 1991.

10. Yura, J.A., Structural Stability Class notes, 1990.

11. Yura, J.A., and Phillips, B., " Bracing Requirements for Elastic Steel Beams", Report No. 1239-1, Center for Transportation Research, University of Texas at Austin, May 1992.